BRNO UNIVERSITY OF TECHNOLOGY

VYSOKÉ UČENÍ TECHNICKÉ V BRNĚ

FACULTY OF MECHANICAL ENGINEERING

FAKULTA STROJNÍHO INŽENÝRSTVÍ

INSTITUTE OF SOLID MECHANICS, MECHATRONICS AND BIOMECHANICS

ÚSTAV MECHANIKY TĚLES, MECHATRONIKY A BIOMECHANIKY

OPTIMIZATION OF CORE MOLDS FOR INJECTION MOLDING

OPTIMALIZACE JÁDRA FORMY NA VSTŘIKOVÁNÍ PLASTŮ

MASTER'S THESIS

DIPLOMOVÁ PRÁCE

AUTHOR — **Bc. Václav Stavárek**

AUTOR PRÁCE

SUPERVISOR — **Ing. Petr Vosynek, Ph.D.**

VEDOUCÍ PRÁCE

BRNO 2019

BRNO UNIVERSITY OF TECHNOLOGY
FACULTY OF MECHANICAL ENGINEERING

Master's Thesis Assignment

Institut:	Institute of Solid Mechanics, Mechatronics and Biomechanics
Student:	**Bc. Václav Stavárek**
Degree programm:	Applied Sciences in Engineering
Branch:	Engineering Mechanics and Biomechanics
Supervisor:	**Ing. Petr Vosynek, Ph.D.**
Academic year:	2018/19

As provided for by the Act No. 111/98 Coll. on higher education institutions and the BUT Study and Examination Regulations, the director of the Institute hereby assigns the following topic of Master's Thesis:

Optimization of core molds for injection molding

Brief description:

The molding core is an important tool for cavity molding when casting plastic connectors. The core is loaded during the cycle by a pressure field caused by an uneven flow of plastic, a temperature field of molten plastic, and some manufacturing inaccuracies. It must be therefore designed to withstand the maximum number of injection cycles. Breaking the core means the downtime of production and also the cost of its repair / new piece. The aim of this work is (in cooperation with an industrial partner) to propose a methodology for estimating the life of the mold core using modern simulation tools.

Master's Thesis goals:

Perform a research study on injection molding of plastics.
Perform simulation of injection molding in a program used in the company (Autodesk Moldflow, Moldex3D).
Use the injection simulation results as the boundary conditions into the ANSYS program and determine the stress-strain fields on the forming core.
Determine the life of the core.
Discuss the possibilities of using the above-mentioned methods when developing new tools and or modifying existing tools.

Recommended bibliography:

KENNEDY, Peter a Rong ZHENG. Flow analysis of injection molds. 2nd edition. Cincinnati: Hanser Publishers, 2013. ISBN 978-1569905128.

KULKARNI, Suhas., [2017], Robust process development and scientific molding: theory and practice. 2nd ed. Cincinnati: Hanser Publications. ISBN 978-1-56990-586-9.

VLK, Miloš, 1992, Dynamická pevnost a životnost. 2., přeprac. vyd. Brno : Vysoké učení technické.

Students are required to submit the thesis within the deadlines stated in the schedule of the academic year 2018/19.

In Brno, 26. 10. 2018

L. S.

prof. Ing. Jindřich Petruška, CSc. Director of the Institute	doc. Ing. Jaroslav Katolický, Ph.D. FME dean

Summary
This thesis was written in cooperation with an industrial company that manufactures electric components for automotive industry. They have issues with frequent core breakage on some of their injection molds, mainly for connector housings. They own licences for injection molding simulation software Moldflow and Moldex3D and also for finite element method simulation software Ansys.

After explaining the essential theoretical background to injection molding and its simulation, fluid-structure interaction problems and fatigue analysis, a complex process of determining fatigue lifetime of injection molding cores with the aid of softwares mentioned above is shown on a specific mold from the production of the company. The fatigue model that describes the current state of the mold the best is then chosen to analyze the influence of changing the core geometry and also injection molding process conditions. Changing other parameters that are not possible to involve in the simulation is also discussed and if possible, justified by using other sources.

One of the recommendations is to add a radius to both of the cores, which could increase the more frequently breaking core's fatigue lifetime from 30 days to more than 320 days. This could mean potential savings of 10 600 EUR every year. The other recommendations are changing the tool machining process and doing an additional heat treatment after the machining.

Keywords polymer injection molding, injection molds, core, insert, lifetime, fatigue, fluid-structure interaction

Rozšířený abstrakt
Tato diplomová práce vznikla v úzké spolupráci s průmyslovým partnerem, který se zabývá výrobou konektorové techniky pro automobilový průmysl. Tématika práce je životnost jader ve formě na vstřikování plastů. Protože výroba těchto nástrojů je velmi nákladná (drahé oceli, drahá výrobní technologie, vysoké nároky na přesnost), je v zájmu firmy konstruovat a provozovat je tak, aby byly jejich životnosti v řádech desítek milionů vstřikovacích cyklů. Některé nástroje toto v současnosti bohužel nesplňují a vznikají tak neočekávané extrémně vysoké náklady na výrobu náhradních jader, což značně zvyšuje cenu výroby daného plastového výlisku. Firma disponuje licencemi na program Ansys (simulace metodou konečných prvků) a Moldflow i Moldex3D (programy na simulaci procesu vstřikování plastů metodou konečných objemů). Potřebovali tedy vypracovat metodiku, jak tyto programy použít k odhadu životnosti jádra a pomocí simulací pak zjistit, který parametr má na životnost největší vliv. Změnou tohoto parametru by pak docílili co možná největšího prodloužení životnosti a z něj plynoucích finančních úspor.

Jádra ve formách na vstřikování plastů jsou při výrobě namáhány nerovnoměrným tlakovým polem roztaveného plastu (převážně ve fázi plnění formy) a také teplotním polem roztaveného plastu. Právě díky tomu, že hlavním zdrojem mechanického namáhání je nerovnoměrně rozložený tlak (plast jádro obtéká), k odhadu deformačně-napěťových stavů nestačí zjednodušený výpočet se zadáním maximální hodnoty tlaku na plochy jádra. K úloze je třeba přistupovat jako ke slabě sdružené interakci kapaliny a tuhého tělesa (tlakové pole plastu ovlivňuje napěťové pole jádra) a nejdříve je třeba co nejpřesněji nasimulovat plnění formy roztaveným plastem. Takto získané tlakové profily lze pak naimportovat jako zatížení konečnoprvkového modelu a zjistit deformačně-napěťové stavy jádra. Z těchto stavů lze pak dále odhadnout životnost jádra pro danou konstrukci a dané parametry procesu vstřikování. V této práci jsou shrnuty teoretické poznatky nutné k takovémuto

odhadu životnosti a také detailně popsaný postup, vysvětlený konkrétně na příkladu jedné formy, ve které se často zalamují jádra.

Je třeba rozlišovat mezi postupným opotřebením nástroje, které je způsobené převážně abrazivním působením skelných vláken v roztaveném polymeru (obsahy vláken se běžně pohybují kolem 15-40 %) a poškozením lomem, které může být způsobené několika faktory. Opotřebení nástroje není narozdíl od lomu tolik obávané, jelikož se s ním počítá při kalkulaci ceny projektu. Mezi hlavní vstupy ovlivňující porušování jader lze řadit: geometrii nástroje, materiál nástroje, postup při výrobě nástroje, tepelné zpracování, povlakování, konstrukce formy jako celku, výrobní tolerance v rámci formy, nerovnoměrné teplotní pole ve formě, druh vstřikovaného plastu, nastavení procesu vstřikování a lidský faktor. Již ze začátku je zmíněno, že simulace není schopna zohlednit postup při výrobě nástroje ani jeho tepelné zpracování či povlakování, výrobní tolerance v rámci formy ani lidský faktor.

Injekční vstřikování je technologie zpracování plastů, výhodná především díky nízkým výrobním časům a možnosti produkovat i geometricky relativně složité tvary. Mezi hlavní procesní parametry patří teploty ohřívačů válce, teplota formy, vstřikovací rychlost, vstřikovací tlak, přepnutí na dotlak, dotlak, čas dotlaku, čas chlazení a dávka. Při vstřikování můžou na výliscích vzniknout různé vady (nedostřik, přestřik, staženiny), které závisí i na těchto parametrech (dále také např. na stavu formy nebo jejím chladícím systému). Většinou pak například nejde při vysoké poruchovosti jader jednoduše snížit vstřikovací rychlost, protože by pak vznikaly samé nedostříknuté kusy. Simulace injekčního vstřikování se využívá hlavně kvůli vysoké ceně nástrojů. Umožňuje totiž předvídat výskyt různých vad, či slabých míst na výlisku a změnit tak zavčas konstrukci výlisku, formy, nebo zvolit jiný materiál ještě v počáteční fázi projektu. Je třeba podotknout, že tento druh simulace se dopouští mnoha zjednodušení, navíc materiálové vlastnosti jsou měřeny v laboratorních podmínkách a vlastnosti materiálu při samotné výrobě se pak můžou lišit. Pokud nás zajímají pouze deformačně-napěťové stavy nástroje, stačí úlohu řešit jako slabě sdruženou (tlak plastu působí na nástroj, ale deformace nástroje nemá vliv na tok plastu). Řešit úlohu jako silně sdruženou by mělo smysl tehdy, pokud by nás zajímal konečný tvar výlisku ovlivněný deformací nástroje.

Byla provedena analýza konkrétní formy vyrábějící desetipozicové housingy na dva různé druhy kontaktů. Jedná se o čtyřnásobnou formu (tzn. vyrábí čtyři kusy najednou při jednom zdvihu nástroje) s horkým vtokem. V poslední době v ní byl detekován vysoký počet poškozených jader zejména na 2 pozicích (531 a 532). Rám formy je z oceli 1.2343 ESU, většina jader je z oceli 1.2344 ESU a dvě nejčastěji se porušující jádra jsou z oceli Vanadis 4 Extra. Pro nedostatek informací v materiálovém listu pro Vanadis 4 Extra proběhla na Fakultě Strojního Inženýrství VUT v Brně tahová zkouška čtyř nenormovaných vzorků poskytnutých nástrojárnou firmy. V zadní části každé kavity formy (na druhé straně od místa, kde tavenina vstupuje), se nachází tlakové čidlo, které měří průběhy tlaků při každém zdvihu a detekuje pomocí nich neshodné výrobky. Spočítané tlaky byly vždy porovnávány s tlaky změřenými z tohoto čidla, aby se ukázalo, jak daleko je simulace vstřikování od reality.

Pro simulaci vstřikovacího procesu byly pro porovnání použity programy Moldflow i Moldex3D. Protože prvotní výsledky byly daleko lepší z Moldex3D, byla v tomto programu vyzkoušena různá nastavení a jejich vliv na výsledný tlak v místě tlakového senzoru. Průběh tohoto tlaku byl srovnáván s reálnými daty z výroby. Výsledky, které se nejvíce přiblížily reálným datům byly při snížení vstřikovací rychlosti v simulaci na 35 $\mathrm{cm^3\,s^{-1}}$ ze 40 $\mathrm{cm^3\,s^{-1}}$, které jsou nastaveny na stroji. Simulace má totiž často tentenci plnit

formu rychleji, protože nezohledňuje nedokonalosti stroje (např. opotřebované těsnění pístu). Dále bylo zjištěno, že zahrnutí lokálního přehřívání formy do simulace pomocí souběžného řešení vedení tepla skrze stěny formy způsobí jen nepatrný pokles tlaku v místě senzoru. I ty nejpřesněji spočítané výsledky předpověděly tlakovou špičku o 20 % vyšší, než byla změřená špička. Tato nepřesnost může být způsobena i pozicí tlakového čidla a zkoumaných jader - jsou v nejvzdálenějším místě od vtoku a právě zde se můžou výsledky simulace nejvíce lišit od reality (tavenina musela urazit velkou vzdálenost, aby zde dotekla).

Další zjištění bylo, že podle simulace dochází při současném nastavení procesu k přepnutí na dotlak až po naplnění 100% objemu formy plastem. K tomuto by na reálném stroji nemělo nikdy dojít, protože to znamená, že píst se snaží obrovskou silou natlačit další plast do už plné formy, což vede k velkému nárůstu potřebné uzavírací síly a možnému poškození nástroje. To, že simulace toto předpověděla, však může být způsobené pouze její odchylkou od reality, která byla vysvětlena výše.

Při aplikaci tlakových profilů jako zatížení v programu Ansys bylo zjištěno, že profily z pozdějších časových okamžiků, kdy už část taveniny začíná tuhnout a výsledky tlaku zde klesají na nulu, způsobují nevěrohodné, vysoké hodnoty napětí a neměly by být používány. V reálu se v místech, kde výsledky klesnou na nulu, nachází ztuhlý plast, který může podepírat nástroj. To, že tento ztuhlý plast má nezanedbatelný vliv na napjatost jádra, bylo dokázáno zjednodušenou simulací s přítomností a bez přítomnosti tohoto ztuhlého plastu. Reálnou úlohu však takto řešit nejde, protože velikost ztuhlé oblasti se mění každý časový krok, tuhnoucí plast se navíc smrskává a jeho chování se stává těžko předvídatelným. Proto byly obě jádra zatíženy jen těmi tlakovými profily, kde ještě v jejich okolí nedocházelo k tuhnutí plastu (zhruba do 0.59 s od začátku cyklu).

Do statického výpočtu metodou konečných prvků byla zahrnuta i okolní jádra, která jsou v kontaktu se dvěma zkoumanými. Kontakty, kde bylo očekáváno možné oddělení ploch, byly definovány bez tření (frictionless), ostatní kontakty jako pevné spojení (bonded). Problémová místa, kde se v reálu vyskytují trhliny, byla vždy zkoumána pomocí submodelů. Úloha byla řešena pro každé jádro s využitím multilineárního i elastického modelu materiálu (oba vytvořené z tahové zkoušky). Mohla tak být spočítána hodnota exponentu m pro odhad amplitudy lokálního celkového přetvoření (elasto-plastického) z pouhého lineárního řešení úlohy (Pospíšilův princip). Byl zkoumán vliv zahrnutí tepelného zatížení části formy teplotními profily získanými rovněž ze simulace vstřikování. Zahrnutí teplotní roztažnosti způsobilo několikanásobný vzrůst špiček přetvoření, což by vedlo k takřka nulové životnosti a tudíž nesouladu modelu s údaji z výroby. První důvod tohoto nesouladu by mohlo být nezahrnutí vůlí mezi jednotlivými jádry formy, které v každé formě musí být z důvodu odvzdušnění (vzduch, který je z kavity vytlačován roztaveným plastem, musí někudy unikat). V reálu možná vlivem tepelné roztažnosti dojde pouze k vymezení těchto vůlí, místo velkého nárůstu přetvoření. Další důvod může být nepřesný odhad koeficientu přestupu tepla mezi plastem a stěnami formy, ten byl v Moldex3D určen automaticky (přesný způsob, jak se při zvolení možnosti "automaticky" koeficient stanovuje, v manuálu programu nebyl uveden). Pokud je použit vyšší koeficient, dojde ke snadnějšímu úniku tepla z roztaveného plastu do stěn formy. Protože viskozita taveniny polymeru závisí i na její teplotě, může to vést k nárůstu odhadnutých vstřikovacích tlaků, což koresponduje s výše popsaným zjištěním, že simulovaná špička tlaku byla vždy minimálně o 20 % vyšší, než ta změřená. Ze snadnějšího úniku tepla do stěn nástroje vyplývá i vyšší odhadnutá teplota nástroje. Ve formě se bohužel nenachází teplotní čidlo a k

dispozici nebylo ani žádné individuální měření teploty nástroje při výrobě (např. kontaktním teploměrem). Nebyla tedy možnost ověřit přesnost spočítaných teplot. Z výše zmíněných těchto důvodů nebylo s vlivem tepelné roztažnosti nadále pracováno. Dále byl zkoumán vliv přenásobení všech zátěžných tlakových profilů koeficientem 0.826, což odpovídá snížení špičky tlaku tak, aby v místě senzoru odpovídala naměřeným datům. Toto způsobilo mírný pokles špiček přetvoření a nárůst životnosti.

Protože v jednom z jader docházelo k lokální plastizaci vrubu, byla únavová životnost stanovena z amplitudy deformace pomocí Manson-Coffinovy křivky. Hodnoty koeficientů této křivky byly stanoveny dle Mansonovy metody univerzálních směrnic. Vliv středního napětí byl zarnut dle Morrowa. Byly vyzkoušeny různé složky středních napětí. Povrch v místě iniciace trhlin byl předpokládán jako broušený a jeho nedokonalost byla zahrnuta koeficientem stavu povrchu 0.81 (byl jím přenásoben první člen Manson-Coffinovy rovnice σ'_f). Jelikož hodnoty exponentu m vycházely pro každý druh zatížení jinak a mimo stanovený interval $(0, 1)$, nebyl Pospíšilův princip použit a místo toho byla úloha pokaždé řešena s multilineárním modelem materiálu. Vstupem do odhadu únavy pak bylo celkové redukované přetvoření ve vrubu podle podmínky HMH. Hodnoty životnosti odpovídající údajům z výroby byly dosaženy při použití zátěžného stavu po přenásobení tlakových profilů koeficientem 0.826 v kombinaci s prvním hlavním napětím jakožto středním. Jádro 532 podle výroby vydrží zhruba 170 000 cyklů, analýzou byla odhadnuta únavová životnost pro současný stav 165 000 cyklů. Jádro 531 vydrží několikanásobně více cyklů (není přesně známo kolik), z analýzy u něj vycházela životnost 2 350 000 cyklů.

S využitím výše zmíněného modelu byl zkoumán vliv velikosti zaoblení v oblasti iniciace trhliny na životnost nástroje. Zaoblování bylo omezeno konstrukcí výlisku i formy. Největší možný poloměr 0.2 mm na jádře 532 by mohl způsobit nárůst počtu cyklů z 165 000 na 1 850 000 cyklů, tj. z 30 dnů výroby na více než 320. Toto prodloužení životnosti se dá vyčíslit na potenciální roční úspory až 10600 EUR (přesná částka závisí na vytíženosti formy v příštích měsících), navíc se v případě úspěchu u této formy dá změna aplikovat i na ostatní formy s podobnými jádry a dosáhnout dalších úspor. Přidání největšího možného poloměru 0.3 mm na vrub jádra 531, kde dochází k iniciaci trhlin, by také snížilo špičku přetvoření a způsobilo prodloužení životnosti ze současně odhadnutých 2 350 000 do oblasti neomezené životnosti.

Dále byl zkoumán vliv změny procesního parametru přepnutí na dotlak ze současných téměř 100% na 90% naplněného objemu formy. Tato změna procesu způsobila jen mírný pokles přetvoření na jádře 532, který by vedl k nárůstu životnosti ze 165 000 na pouhých 190 000, což je z hlediska běžného rozptylu únavových dat zanedbatelná změna. Navíc by se dřívějším přepnutím na dotlak prodloužil vstřikovací cyklus o několik desetin sekundy, což by vedlo ke zdražení výroby. Změna tohoto procesního parametru tedy nebyla navrhnuta.

Na závěr byl uveden souhrn doporučení pro konstruktéry nástrojů, nástrojaře a technology. Pro prodloužení životnosti nástroje není zapotřebí vždy provádět komplikovanou simulaci interakce tělesa a tekutiny. Tato simulace zabere mnoho času a její výsledky často nemají hodnotu, která by tento čas vyvážila. Když se na nějakém jádře začnou objevovat trhliny, je třeba zjistit přesné místo jejich iniciace, toto místo pak co nejvíce zaoblit (tento krok je bohužel často omezen konstrukcí výlisku a formy) a snížit tak koncentraci napětí. Pokud toto nepomůže, je třeba se zaměřit na výrobní proces nástroje (v tomto případě elektrojiskrové obrábění). Jde zejména o nastavení řezu - pokud nějaká plocha netvoří plochu na výlisku, je často obráběna menším počtem řezů a má pak horší

drsnost povrchu. Pokud se právě na této ploše iniciuje trhlina, je třeba zvážit, zda ji neobrábět také větším počtem řezů. Dále lze po obrábění přidat popouštění pro snížení zbytkových napětí dle pokynů dodavatele. Dalším krokem může být přidání ochranného povlaku, či změna procesních parametrů jako snížení vstřikovací rychlosti, dřívější přepnutí na dotlak, nebo snížení dotlaku, každá změna procesního parametru však musí být otestována přímo ve výrobě, aby se zjistilo, zda nezpůsobuje vady na výlisku.

Klíčová slova injekční vstřikování plastů, formy na vstřikování plastů, jádro, vložka, životnost, únava, interakce tělesa s tekutinou

Bibliographic citation

STAVÁREK, V. *Optimization of core molds for injection molding.* Brno: Brno University of Technology, Faculty of Mechanical Engineering, 2019. 51 p. Supervisor Ing. Petr Vosynek, Ph.D.

I declare that I have written this master's thesis Optimization of core molds for injection molding on my own according to the instructions of my master's thesis supervisor Ing. Petr Vosynek, Ph.D., and using the sources listed in references.

Bc. Václav Stavárek

I would like to express my thanks to my master's thesis supervisor Ing. Petr Vosynek, Ph.D., from Institute of Solid Mechanics, Mechatronics and Biomechanics, Brno University of Technology, for his guidance and advices during the process of writing this thesis and also for performing the tensile test for this thesis in his free time. I would also like to thank my colleague Viktor Čech for making this thesis possible, people from our tool shop for manufacturing the specimen, Vlastimil Tegza and Matthias Hoch for their advices about tooling manufacturing, Pavel Bureš, Bohuslav Máša and the whole mold design team for their advices about tool design, Vladimír Buřt and other technologists for answering my questions about injection molding process, Mahesh Nichite for inspiring me with the topic, Tham Nguyen-Chung for answering my questions about injection molding simulation. My last thanks goes to my family and friends who supported me during my studies.

Bc. Václav Stavárek

Contents

1. Introduction

When molding thin walled, complex shape plastic parts such as fuseboxes or connector housings, high injection pressure is required (specialized machines can deliver up to 250 MPa) [4]. This high pressure brings several complications to this process. The uneven polymer flow can cause excessive deflection of the core (core shift) which means wrong dimensions on the final product. To prevent this core shift, different types of arretation are used to make the core more rigid. However, there is lot of mechanical stress acting on these cores and their arretations. Because injection molding is a periodic process, the core can easily fail due to fatigue even for stresses below its yield strength.

On a technical conference in 2016 held by the company, our colleagues from Germany presented a report on injection mold core design change using CAE approach from [3]. The new design has been first applied on a mold in Belgium. In one year, core breakage incidents on this mold were drastically reduced which led to a big annual saving. After first succesful implementation, without any further simulations they also applied the design to 2 identical molds in Germany. Core breakage incidents on these 2 molds were reduced by more than 90% which meant even bigger annual saving. A significant total annual saving was achieved by one injection mold core design change. At the end of the report they were pointing out the possibility of implementing this approach all over the EMEA region with potential opportunities for huge savings.

Couple of months after the conference one of the colleagues visited the company's plant in Kuřim and presented this idea to local Mold Design and Tool & Die departments. Since core breakage is a big issue in this plant as well, a master's thesis assignment was created to study core breakage with the aid of CAE.

2. Core breakage problem

An industrial company that manufactures electric components for automotive industry has requested this thesis to solve their issues with one of the most problematic molds. The cores in this mold have a very short service life and there are high annual costs just for its repairs. The company has licences for commercial softwares for injection molding simulation Moldflow and Moldex3D and also for FEM simulation Ansys, therefore using these programs was strongly recommended.

2.1. Objectives of the thesis

Since the tooling for small and accurately molded parts has to be manufactured by fairly expensive technologies, the effort is to design the whole tool with as high service life as possible. Objectives of this thesis are:

1. Simulate the injection molding process using Moldflow or Moldex3D to get pressure and temperature results at cores surfaces.
2. Use those results as boundary conditions in Ansys to calculate the peak strains and stresses at core crack initiation areas.
3. Predict the fatigue lifetime of the problematic cores. If possible, the results should be corresponding with information about actual lifetime of the cores in production.
4. Use the first 3 steps to assess the influence of some factors from section 2.2 on the service life of the cores. Propose some changes that could lead to increase of the cores service life and therefore savings on mold repairs.

2.2. Factors influencing premature core breakage

First, we need to distinguish between regular tool wear and premature breakage.

Tool wear is something that occurs in every mold. The tool gets gradually abraded by repetitive polymer injection and ejection, changes its dimensions and is not usable anymore. It is mainly influenced by factors such as tool material, tool surface treatment or coating and % of glass fibre in the polymer. It is not such a dreaded phenomenon since this is usually taken into account when calculating production project costs. Worn out tools are being replaced within TPM to prevent line stops.

Core breakage, unlike tool wear, happens instantly and is something that was usually not accounted for. It can not be treated within TPM, because its occurence is more random. Cores usually undergo low or high cycle fatigue failure, because they're exposed to high amount of mechanical stress. This stress can be related to uneven polymer melt pressure across core surfaces. The main factors that influence premature core breakage would be:

Core geometry Core has sharp notches that cause stress concentrations or is just too thin and long. Some of these geometries can be fixed while others form geometrical features on the molded product, meaning that product design change would be required to remove them.

Core material Material with too low fatigue strength was chosen for the tool.

Core manufacturing process Manufacturing processes such as EDM (commonly used for small cores) or SLS (used for cores with conformal cooling channels) can affect the tool fatigue strength. This will be discussed in section 5.4.

Core heat treatment and coating The influence of heat treatment and coating of tool on its fatigue strength will be discussed in section 5.5

Mold design The mold itself can be sometimes poorly designed and causing strongly uneven pressure distribution on cores. Changing the gate location or adding another gate to make the filling more balanced could help in this case.

Mold tolerances When the tolerances on the mold drawing are set wrong or the mold is manufactured out of tolerances, collision between the cores on two halves of the mold can occur. This could cause faster tool wear and also core breakage.

Uneven mold temperature The mold is held at constant temperature by system of cooling circuits. However, there still are some temperature gradients inside that can cause thermal stresses and help crack initiation and propagation. These stresses are fluctuating throughout the injection molding cycle.

Polymer material When the polymer is too viscous in its molten state, higher injection pressure is required which means there's more stress on the core. On the other hand, if we wanted to change the material, the replacement material would have to have comparable mechanical and electrical properties as the original one to pass all the product validation tests (such as LV214).

Injection molding process parameters In [2] it was shown that the injection pressure is the dominant process parameter affecting core shift and core stress. Other process parameters that could be adjusted are discussed in subsection 3.1.1. However, changing process parameters can cause other problems which will be explained in subsection 3.1.2.

Human factor Even though the injection molding process is highly automated, human error can still influence core breakage. For example when the molded product gets stuck in the mold and can't be ejected the machine detects it and doesn't close the mold again. It sometimes happens that the operator does not notice the stuck product and tries to close the mold, causing high stress on the mold and cores.

Predicting the core fatigue life by using simulations can help to determine which factor is the most important one in each case of core breakage. However, these simulations are not able to describe effect core manufacturing process, core heat treatment and coating, mold tolerances or human factor. Core manufacturing process and its resulting surface roughness can be partially taken into account in fatigue estimation. For molds that are already running in the production it is often impossible to completely change the mold design (for example add new gates) just to prevent core breakage, therefore it is required to look for small changes that would not bring too many additional costs for mold rework.

2.3. Mold selection

Our local toolmakers prepared a list of molds with biggest costs for spare cores during the last year. From this list we picked the mold 1857138 which has two cores on positions 531 and 532 that frequently break during production. Manufacturing cost for core 531 is 320 EUR and for core 532 it is 240 EUR. Not only that their repairs increase COPQ significantly, but similar core designs are also used in other molds across the company. Further information about this mold can be found in chapter 6.

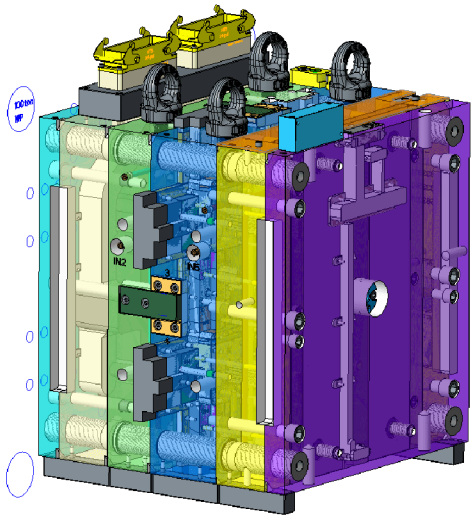

Figure 2.1: Problematic mold 1857138

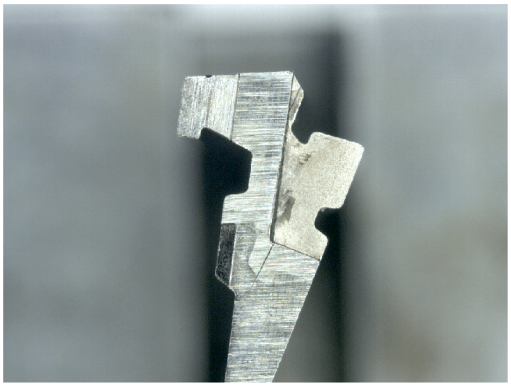

Figure 2.2: Damaged core 531

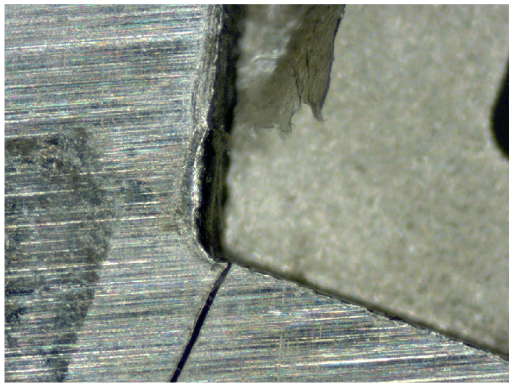

Figure 2.3: Fatigue crack on core 531

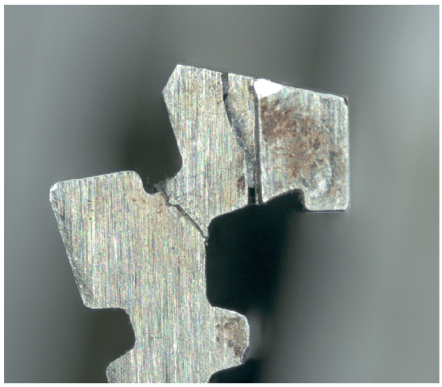

Figure 2.4: Damaged core 532

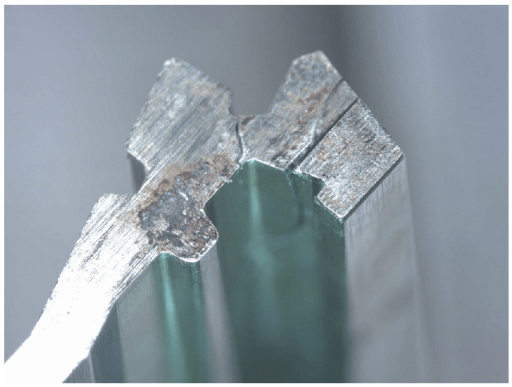

Figure 2.5: Fatigue cracks on core 532

3. Injection molding

Injection molding is a polymer processing technology frequently used in automotive and consumer electronics industries. Its main benefits are fast production rates and freedom to produce complex 3D geometries.

Figure 3.1: Injection molding machine with horizontal clamp and horizontal injection, Arburg Inc. [5]

First, raw material in form of plastic pellets is fed into the injection molding machine (figure 3.1) barrel, where the plastic is melted primarily by shear heat generated from the rotating screw but also by external electric heating bands. As the screw rotates, it accumulates the required amount of plastic for the shot to the front of the barrel. The forward movement of the screw then injects this plastic into the mold. Mostly there are some channels in the mold that have coolant flowing through them to help maintain the desired mold temperature. When the part gets cooled below its ejection temperature, it is ejected out of the mold.

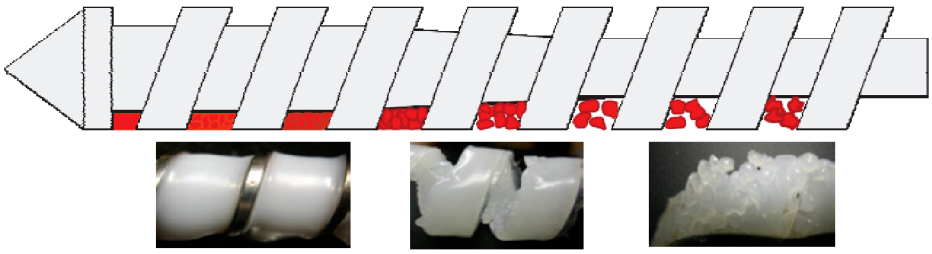

Figure 3.2: Melting progression of the plastic as it travels through the sections of the screw [5]

In [4] it was said, that the whole process can be divided into following phases:

1. Mold closing: Injection and ejection halves of the mold are connected, clamping force is applied.

2. Filling or injection: Molten polymer is filling the mold cavity or cavities.

3. Packing and holding: Certain pressure is maintained in the cavity, more melt enters it to compensate for shrinkage during cooling and solidification.
4. Cooling: Part is being cooled until it is mechanically strong enough to be ejected out of the mold.
5. Plastication and screw back: New dose of polymer material is being plasticized.
6. Ejection: Finished part is ejected out of the mold.

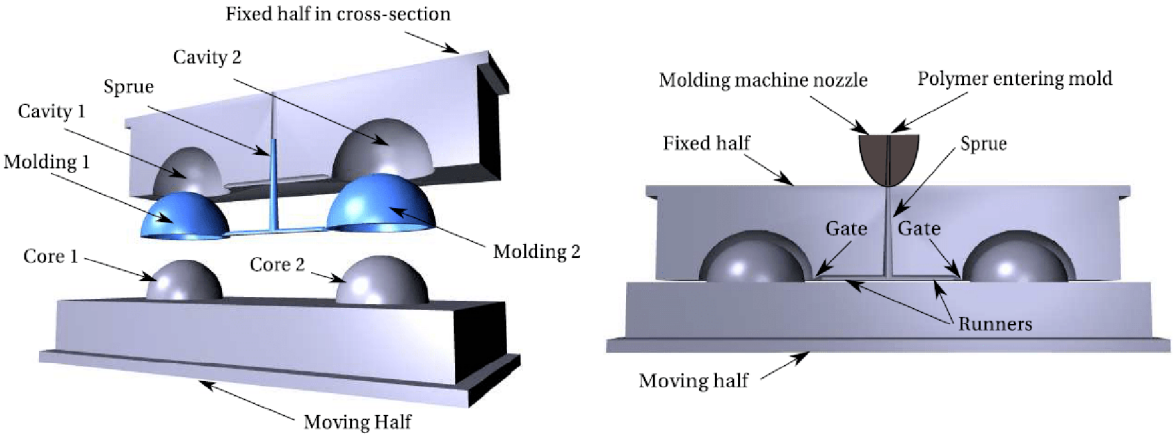

Figure 3.3: Mold parts [4]

The mold itself can then be divided into following parts [4]:

- Injection or fixed half: Is fixed to the machine.
- Ejection or moving half: Is moving in one direction either to form the cavity or allow ejection of the part.
- Cavity: The hollow space in the mold to be filled with polymer. If the mold has multiple cavities it means that multiple parts can be produced in one cycle.
- Core: Tool in the mold that forms internal holes etc. in the part. The part usually shrinks onto it and needs to be detached from it by ejector pins after the mold opens.
- Sprue: The channel that brings melt from the injection machine to the mold
- Runner: The channel that transfers melt from the sprue to the cavities
- Gate: A channel much smaller in diameter than the runner. Makes removal of the molded part from the runner system easier.

3.1. Injection molding process

The molding process has been traditionally defined only as the inputs to the molding machine, which is not a sufficient definition. According to [5], the word process should actually mean everything that happens to the plastic material from when it enters the plant as a granulate until it leaves the plant as a molded product. For example storage of the raw material and its drying both have significant influence on the final product quality.

3.1.1. Molding parameters

In this thesis, only those parameters from [5] that are inputs to the molding machine and commercial simulation software will be analyzed. All of those parameters and histories of their changes should be recorded in process sheets. They are all related to speed, pressure, time and temperature.

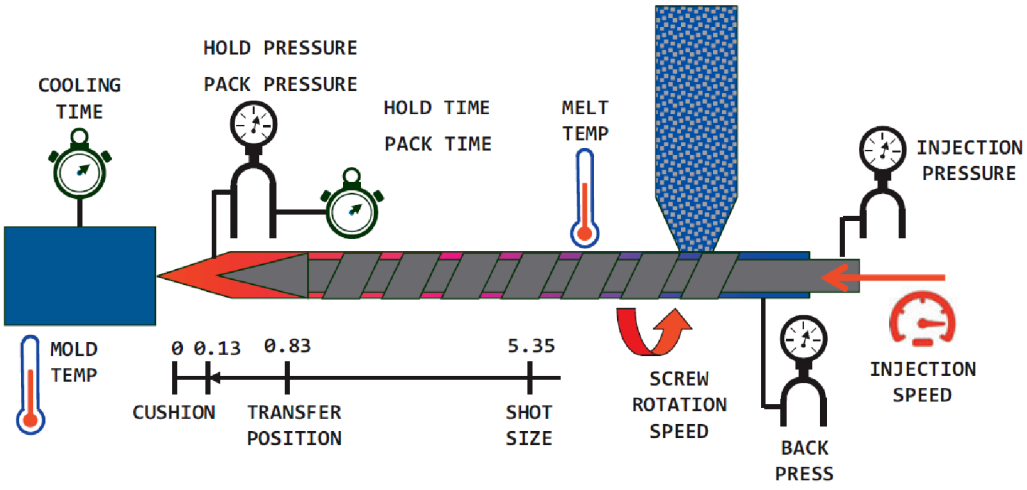

Figure 3.4: Plastic injection molding parameters [5]

Barrel temperatures Temperatures of the heaters around the barrel that help to achieve the desired melt temperature. Depending on the length of the barrel there can be more heater bands. The temperature is usually set higher for those close to the end of the barrel where the polymer should be at temperature ready for injection.

Mold temperatures Heat from the molten polymer escapes the cavity mainly by conduction through mold walls. Mold temperature is set by flow of heat transfer fluid (water for mold temperatures below 100°C and oil for higher temperatures) through cooling channels.

Injection speed The speed of linear screw motion during filling. It can be defined as flow rate in $\mathrm{cm}^3\,\mathrm{s}^{-1}$ or screw speed in $\mathrm{mm}\,\mathrm{s}^{-1}$, these two definitions are related to each other through screw diameter.

Injection pressure The pressure applied to the machine screw to achieve the set injection speed.

Transfer position or velocity/pressure switch-over The point of transfer from injection to packing and holding phase. It can be defined by position of the screw, volume of polymer injected, time or hydraulic pressure. Theoretically the transfer should come when 100 % of the cavity volume is filled but in reality it comes earlier.

Packing pressure The pressure applied during first subphase of packing and holding. Additional polymer is packed into the cavity to compensate for shrinkage that will take place. This parameter is very important because it affects shrinkage and final dimensions of the part.

Packing time The time for which the packing pressure is applied.

Holding pressure The pressure applied during second subphase of packing and holding. This pressure makes sure that no overflow of plastic goes to the cavity nor does the plastic flow back out of the cavity.

Holding time The time for which the holding pressure is applied. It should be optimized to end just after the polymer in the gate solidifies (gate freeze).

Cooling time The time for which the mold is kept closed until the polymer cools down to ejection temperature. It is important to distinguish between set cooling time and actual cooling time because the plastic starts to cool off at the moment it touches the cavity. Therefore the actual cooling time would be injection time + packing time + holding time + set cooling time.

Shot size When the screw is all the way in its forward position after injection, we call this the zero position. The distance that the screw travels back to pick up new dose of material is called the shot size. It is defined in terms of volume. Shot size can be estimated from total shot weight and melt density of the plastic, but can't be calculated exactly because melt density is temperature dependent and exact temperature of the melt is difficult to determine. Some additional material (cushion) also needs to be added for packing and holding phase.

3.1.2. Common defects on injection molded parts

There are numerous defects that can occur on parts manufactured by injection molding. They can be caused by part design, part material, mold design, choice of molding machine but also by the molding process itself. Therefore if we were planning to change some of the parameters in 3.1.1 to prevent core breakage, the parts coming out of the modified process need to be checked for such defects and their dimensions also need to be inspected.

Some common defects on molded parts and their possible causes named in [5] are listed below. With enough knowledge about the process they can be predicted in the simulation software.

Short shot Molten plastic does not reach the back of the cavity.

- Melt temperature too low

- Mold temperature too low
- Injection speed too low
- Insufficient venting in the short shot area
- Gate or runner diameters are too small

Flash Molten plastic flows beyond the cavity.

- Mold damaged
- Melt temperature too high
- Mold temperature too high
- Injection speed too high

Sink Shrinkage is not being compensated by additional polymer which results in sink marks

- Packing and holding pressures too low
- Packing and holding times too short
- Melt temperature too high
- Mold temperature too high

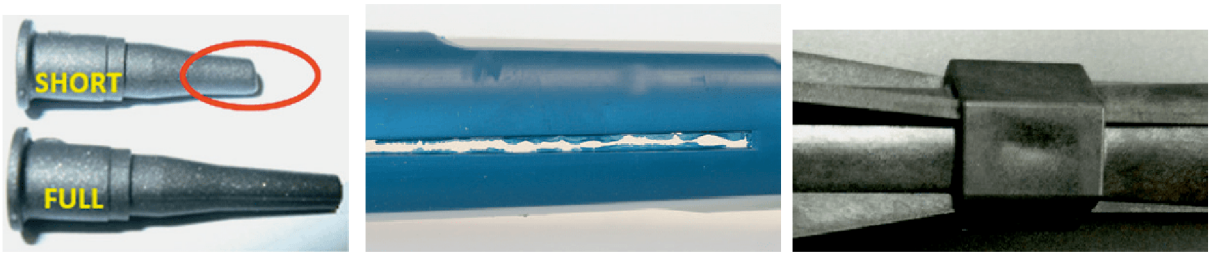

Figure 3.5: From left to right: Short shot, flash and sink marks [5]

Now we can see that by decreasing injection pressure or packing pressure to prevent core breakage we can introduce short shot or sink mark defects to the part. We should adjust some parameter only when we're able to compensate the induced change in product by changing some other parameters.

3.2. Injection molding simulation

Defined in [4], injection molding simulation involves using a computer to solve a set of equations and their associated boundary conditions, that represent a mathematical model of the molding process. This leads to a huge amount of data usually displayed in form of colored plots of particular variable. Because the cost of tooling for injection molding is high, it is good to perform simulations in the early stages of product and mold design to evaluate different options in terms of part and mold designs and materials.

According to [4], most effort has been devoted to simulation of these phases:

Filling Is characterized by high flow and shear rates. Convection of the melt is dominant heat transfer mechanism in this phase. Additional heat can be generated by viscous dissipation. A thin layer of solidified material called frozen layer is formed at cavity walls, if it gets thicker it obstructs the incoming polymer flow and requires higher injection pressure to fill the cavity.

Packing and holding Cavity is full, remaining polymer flow is only compensating shrinkage, therefore convection and dissipation become minor effects (except gates and thin to thick region transitions). Conduction of heat is the major heat transfer mechanism. At gate freeze the cavity gets isolated from the applied pressure. Sometimes the material can loose contact with the mold wall during this phase, this condition significantly complicates calculation of temperature of the material in the cavity.

Cooling Similar process physics as at the end of holding.

It is obvious that simulating this manufacturing technology is not an easy task. The process involves several heat transfer mechanisms, it is transient, it deals with a flow of a compressible non-Newtonian fluid, a phase change and it has time-dependent boundary conditions. Other complications are material properties and geometric complexity of the mold.

3.2.1. Material properties of polymers

As said in [4], polymers can be divided by molecular structure to:

Thermoplastic This type of polymer consists of molecular chains that are strong by themselves, but connected to each other just by weak intermolecular forces . They melt above a specific temperature and solidify when cooled down. They can be reshaped when repeatedly heated up. In solid state they are less stiff and strong, but more tough than thermosets.

Thermoset Raw thermosetting polymers are fluid, but when the temperature increases, unlike for thermoplastics, their molecular chains create strong interconnections. This reaction is also called cross-linking. If the material is heated up again, it burns instead of remelting. In solid state they are stronger and stiffer, but less tough than thermoplastics.

Both thermoplastic and thermoset materials can be injection molded. However, this thesis will be focused on thermoplastic injection molding and its simulation.

According to [4], by nature of their solidification, polymers can also be divided to:

Amorphous For amorphous polymers, the entanglement of molecular chains created in molten phase is preserved during their solidification. When they are cooled down, they first become rubbery and below their glass transition temperature they become a hard glass-like material.

Semi-Crystalline For crystallizable materials it is possible that the molecules align themselves during their solidification. Semi-crystalline polymers will form randomly

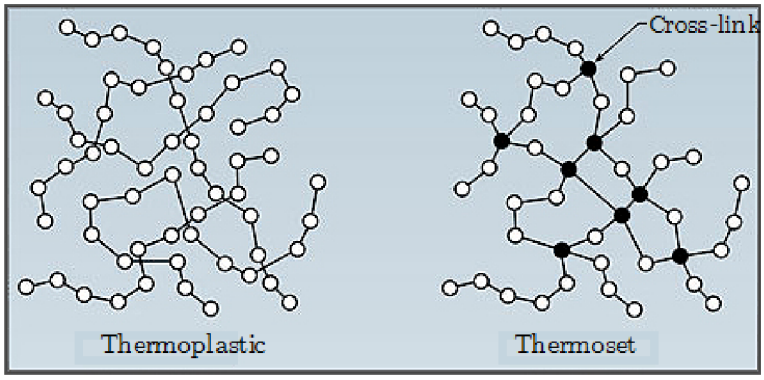

Figure 3.6: Difference in molecular structures of thermoplastics and thermosets [8]

oriented amorphous and crystalline regions when cooled down. Slower cooling generally causes higher crystallinity and fast cooling decreases the level of crystallinity. Crystallization is also affected by deformation rate, which is a big challenge for injection molding simulation of semi-crystalline materials.

In this chapter I will discuss material properties required to simulate injection molding. It must be noted that those properties change during the process and that they are mostly measured under laboratory conditions that differ from conditions in the molding plant, which brings intrinsic errors to the simulation.

Stated in [4], to do a flow analysis (filling, packing and cooling), we need to know following properties:

Viscosity [$\mathrm{N\,s\,m^{-2}}$] Polymer melt is viscoelastic in nature, but using viscoelastic material models would complicate the analysis too much. In simulation, polymers are assumed to be generalized Newtonian fluid. Polymer melt viscosity generally decreases when the material is sheared. This phenomenon is called shear thinning. The viscosity also decreases with increasing temperature. There is number of models that incorporate shear thinning and temperature dependence of viscosity into simulation. The most frequently used ones can be found in [4].

Specific heat capacity [$\mathrm{J\,kg^{-1}\,K^{-1}}$] Measure of how much energy is stored in a material at a certain temperature. This is the dominant property during convection of heat into the mold (filling phase). It can be measured under constant volume (c_v) or constant pressure (c_p, more common). It is also used to calculate heat generated by viscous dissipation. Specific heat of polymers is generally much higher than specific heat of metals, but the amount of heat removed from mold is defined as product of specific heat capacity and density and metals density are an order of magnitude higher than density of polymers.

Thermal conductivity [$\mathrm{W\,m^{-1}\,K^{-1}}$] Thermal conductivities of polymer and mold materials are required. Compared to metals, polymers generally have much lower thermal conductivities. That is why this property is difficult to measure for polymers.

Expansivity [$\mathrm{K^{-1}}$] Also called coefficient of volume expansion. It relates change of volume with change of temperature for constant pressure.

Compressibility [$m^2\,N^{-1}$] Also known as isothermal compressibility coefficient. Relates change of volume with change of pressure for constant temperature.

Pressure-Volume-Temperature Data It is usually provided in form of specific volume as a function of pressure and temperature (PVT diagram). Expansivity, compressibility and also density are obtained from this diagram. The data is obtained by high pressure dilatometry, which is extremely challenging and difficult experimental technology.

No-Flow temperature Or also transition temperature, was introduced by Moldflow. At this temperature the material is assumed not to flow. Below no-flow temperature, extremely high viscosity is assigned to the material. Using a single value for transition temperature introduces some error when simulating semi-crystalline materials, because their crystallization depends on deformation rate and cooling rate.

To simulate shrinkage and warpage, we need to do a fiber-orientation analysis (models used for this analysis can be found in [4]). We also need to know linear coefficients of expansion in directions 1 and 2 and linear elastic data such as Young's modulus and Poisson's ratios in directions 1 and 2.

The properties listed and used in commercial simulation software are either provided by resin suppliers, measured in software developper's CAE lab, taken from CAMPUS plastics database or taken from literature. It is not recommended to use crucial material properties from unreliable sources.

3.2.2. Methods of injection molding simulation

All the governing equations (conservation of mass, conservation of momentum and conservation of energy), their approximations for injection molding and their integration can be found in [4]. In this chapter I will discuss the discretion methods used in today's commercial codes, because these are the options in simulation software that the user has to choose from and should be familiar with.

Midplane This approach takes advantage of the fact, that pressure varies significantly over the molding, but is almost constant across mold thickness, while temperature changes a lot across the mold thickness (this does not apply to bulky parts). Pressure is then solved by finite element method only in two dimensions on the surface of the part and temperature is solved by finite difference method in three dimensions. It is also frequently called the 2.5D approach. Midplane method was most popular between 1980 and 1997, because it saves computational time and also because CAD systems in that time were surface-based. If we want to use this method for 3D CAD model, the midplane must be extracted from the model. There are three variables at each node – pressure p, fluidity S_2 and temperature T.

Dual Domain It is an improved version of midplane analysis. No midplane needs to be generated, the external surface mesh on 3D geometry is used instead. Certain thickness is defined for these surface elements. Connector elements have to be added at some locations of the mesh to make the material flow simultaneously along the

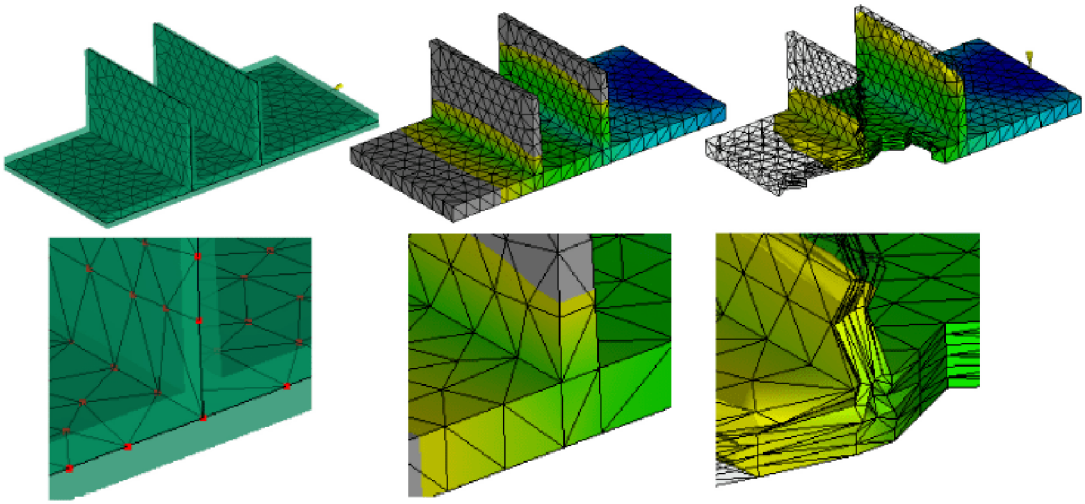

Figure 3.7: From left to right meshes for midplane, dual domain and full 3D analysis in Moldflow [6]

top and bottom surfaces. We are technically performing two analyses, one on each side of the mesh. This means we also need more computational time compared to midplane analysis, but we are saving time that would be needed for midplane model preparation. This technology was patented by Moldflow and is used exlusively by them. The amount of variables at each node is the same as for midplane – pressure p, fluidity S_2 and temperature T.

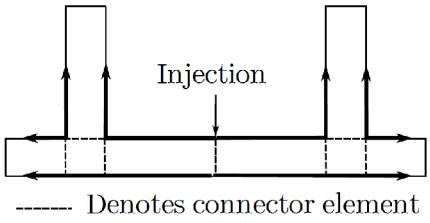

Figure 3.8: Dual domain analysis principle shown on cross section of a part with two ribs [4]

3D analysis This type of analysis should be the ultimate method of simulation because it avoids the 2.5D approximation – there is no restriction on the thickness of the part, the whole computational domain is meshed with tetrahedral or hexahedral elements. Most injection molded parts are thin walled and have huge temperature gradients in the thickness direction. This complicates 3D analysis because it means many elements have to be used across the part thickness. The 3D mesh can have boundary layers of prismatic elements to capture these gradients better (figure 3.9). The total number of elements for 3D analysis increases dramatically compared to midplane or dual domain analyses and therefore the computational time is much

higher. At each node we have five variables – pressure p, temperature T, and three components of velocity v_x, v_y and v_z.

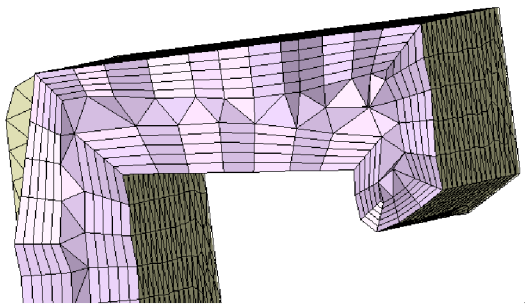

Figure 3.9: Boundary layer mesh used in Moldex3D

4. Fluid-Structure Interaction

The phenomenon of interaction between fluids and solids can be seen everywhere around us (deformation of trees caused by wind, erosion of rocks caused by flowing water). Sometimes it is necessary to understand this process, for example to avoid buildings collapsing in strong wind. Fluid-structure interaction (FSI) problems were defined by Zienkiewicz and Taylor in [7]:

> "Coupled systems and formulations are those applicable to multiple domains and dependent variables which usually describe different physical phenomena and in which neither domain can be solved while separated from the other and neither set of dependent variables can be explicitly eliminated at the differential equation level."

According to [9], there are two different approaches to solving FSI problems.

4.1. One-way coupling

The first one is called one-way coupling (figure 4.1a). At the beginning, the fluid field is solved, from which we obtain forces at the structure boundary. These forces are then transferred as boundary conditions for the structural field. When the structural part gets solved, we repeat this process for the next time step. One-way coupling is suitable for situations where one field is strongly influencing the other one, but not the opposite way. Its benefits are lower computational time and no deformation on the fluid mesh which means constant quality of the mesh.

As it was already shown in [3] and [1] if we are interested in how does the polymer melt pressure affect the stresses in the mold and its cores, we need to analyze it as a one-way coupled FSI problem. One way coupling is sufficient in this case, because the mold deflection is usually in orders of hundredths of milimeters, which is not enough to alter the polymer pressure distribution significantly.

4.2. Two-way coupling

In two-way coupling (figure 4.1b), we solve the fluid field and transfer the obtained forces at the structure boundary to the structural field. The response of the structure to this load is some kind of displacement. The displacement at the structure boundary is interpolated to the fluid mesh and causes its deformation. For the next time step the fluid part of the problem is solved on a deformed mesh. Two-way coupling is suitable for situations where both fields influence each other. This type of solution is more accurate and it guarantees energy conservation at the interface. Cost of this is significantly higher computational time.

If we wanted to determine the molded part final dimensions affected by core shift and mold deflection, two-way coupling would have to be used.

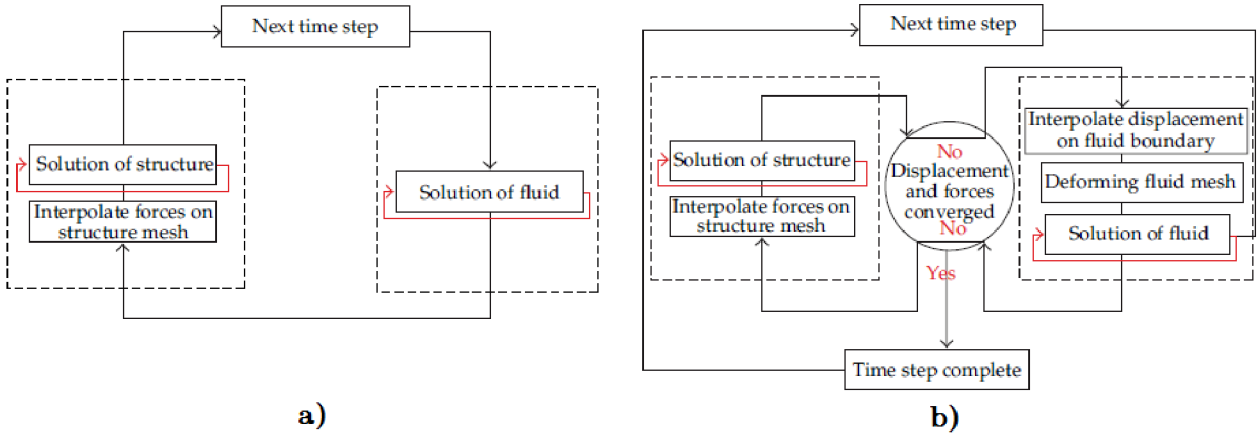

Figure 4.1: Solution procedures for a) One-way coupled problem b) Two-way coupled problem [9]

5. Fatigue

As in [10], there are two stages of fatigue lifetime of structures:

1. Crack nucleation: characterized by fatigue curve, can be divided into substages of changes of mechanical properties, microcrack nucleation and microcrack growth.
2. Crack growth: characterized by fracture mechanics, can be divided into substages of macrocrack growth and final breakage.

For injection molding cores, all cracks are unacceptable. When any crack is visually detected, the core has to be replaced. This means that using fatigue curve is sufficient in this case. Fatigue assessment methods can be divided to:

- Low cycle fatigue: crack nucleation occurs mainly on grain boundaries and is characterized by strain-life curves (Manson-Coffin – eq. 5.1), crack growth is described by elastic-plastic fracture mechanics.

$$\varepsilon_a = \frac{\sigma'_f}{E}(2N)^b + \varepsilon'_f(2N)^c \tag{5.1}$$

  Where ε_a is the total strain amplitude, σ'_f is the fatigue strength coefficient, b is the fatigue strength exponent, ε'_f is the fatigue ductility coefficient, c is the fatigue ductility exponent and $2N$ is the number of reversals to failure.

- High cycle fatigue: crack nucleation occurs in crystallographic slip planes and is characterized by stress-life curves (Basquin – eq. 5.2, Wöhler), crack growth is described by linear elastic fracture mechanics.

$$\sigma_a = \sigma'_f(2N)^b \tag{5.2}$$

The choice between using strain-life or stress-life curve usually depends on factors like expected number of cycles (strain-life for 10^3 to 10^4 cycles, stress-life for 10^6 to 10^7 cycles), amount of plastic deformation during one cycle (strain-life for big plastic deformation) or the behavior of loading (strain-life for hard loading with constant strain amplitude, stress-life for soft loading with constant stress amplitude).

5.1. Fatigue parameters estimation

For many materials, parameters σ'_f, ε'_f, b and c can not be found in their data sheet. Since carrying out fatigue tests to determine those can be lengthy and expensive process, it is needed to estimate them from other mechanical properties that can be found in the data sheet. In [16], two methods are shown to estimate fatigue parameters from other parameters that are easier to obtain such as ultimate tensile strength (R_m), Young's modulus (E) and strain at fracture (ε_f). The first one is universal slopes method by Manson and the second one is a method by Bäumel and Seeger which applies to low-alloy steels. The method by Bäumel and Seeger also estimates values of K' (cyclic strength

Table 5.1: Fatigue parameters estimation according to Bäumel and Seeger [16]

Parameter	Manson	Bäumel and Seeger
σ'_f	$1.9018 \cdot R_m$	$1.5 \cdot R_m$
b	-0.12	-0.087
ε'_f	$0.7579 \cdot \varepsilon_f^{0.6}$	$0.59 \cdot \psi$
c	-0.6	-0.58
ψ	–	1 for $\frac{R_m}{E} \leq 3 \cdot 10^{-3}$ $(1.375 - 125 \cdot \frac{R_m}{E})$ for $\frac{R_m}{E} > 3 \cdot 10^{-3}$)
K'	-	$1.65 \cdot R_m$
n'	-	0.15

coefficient) and n' (cyclic strain hardening exponent). Both methods are shown in table 5.1.

However, it is important to be aware that estimation of these parameters can't ever replace the fatigue tests, necessary for some applications such as aviation industry.

5.2. Generalized Neuber rule

Pospíšil has introduced a method of estimating localized stresses and strains in areas where yielding occurs [16]. It uses fictional elastic stress from linear analysis as an input.

$$\sigma_{fic} = E \cdot {\varepsilon_e}^m \cdot {\varepsilon_t}^{(1-m)} \tag{5.3}$$

Where σ_{fic} is the fictional stress from linear elastic analysis, E is the Young's modulus, ε_e is the actual elastic strain in the yield area, ε_t is the actual total strain in the yield area and m is the exponent characterizing the type of load case.

Different values of exponent m:

- $m = 0$ for hard loading, deformation evenly distributed through section
- $m = 1$ for soft loading, stress evenly distributed through section
- $m = 0.1$ for hard loading out of notches, e.g. thermal stress
- $m = 0.5$ for notches with both soft and hard loading (Neuber rule)
- $m = 0.6$ for soft loading, stress unevenly distributed through section

According to [18], equation 5.3 has 2 unknown variables and to solve them, additional constitutive relationship is needed. In case of uniaxial loading, Ramberg-Osgood relationship can be used. Ansys fatigue module uses the Masing model:

$$\Delta\varepsilon = \frac{\Delta\sigma}{E} + 2\left(\frac{\Delta\sigma}{2K'}\right)^{\frac{1}{n'}} \tag{5.4}$$

The common procedure recommended in [16] is to solve the problem as linear and also as nonlinear to obtain both fictional stress and actual elastic and total strain in the

notch. The value of exponent m is then calculated from equation 5.5 (derived from 5.3) and used in Generalized Neuber rule during further linear solutions. This approach has the main benefit of avoiding repeated time-consuming nonlinear solution. Ansys fatigue tolbox always works with Neuber rule ($m = 0.5$), therefore it should only be used for load cases where $m \approx 0.5$.

$$m = \frac{\ln \sigma_{fic} - \ln E - \ln \varepsilon_t}{\ln \varepsilon_e - \ln \varepsilon_t} \tag{5.5}$$

5.3. Effect of load cycle assymetry

As said in [10], non-zero positive value of mean stress affects the fatigue process. It shortens crack nucleation and also the crack growth phases.

According to [16], effect of mean strain value in low cycle fatigue can be neglected. However, effect of mean stress should be considered in both high and low cycle fatigue. In the same source they introduced modifications of Manson-Coffin and Basquin curves established by Morrow (5.6 and 5.7).

$$\varepsilon_a = \frac{\sigma'_f - \sigma_m}{E}(2N)^b + \varepsilon'_f(2N)^c \tag{5.6}$$

$$\sigma_a = (\sigma'_f - \sigma_m)(2N)^b \tag{5.7}$$

Where σ_m is the mean stress.

5.4. Effect of manufacturing technology

The manufacturing technology by which the tool is made has not negligible effect on the tool's fatigue performance. The main manufacturing technology used for small injection molding cores is electric discharge machining (EDM).

In electric discharge machining, the material is removed by series of electrical sparks between the tool (electrode) and workpiece. An advantage of this technology is the possibility to produce geometrically relatively accurate and complex shapes independently of the workpiece hardness, as long as it conducts electricity. Disadvantage is that these sparks are forming pits in the workpiece surface that induce stress concentrations. The material is basically burnt away, which also means there are residual stresses due to uneven heating and heat-affected zone after EDM machining. According to [13], the main parameters influencing fatigue life of the workpiece are:

Tool polarity The electrical polarization of the tool and workpiece is affecting machining performance and final surface roughness. Positive polarity of the tool is called reverse polarity (r.p. in figure 5.3) and it offers a better surface finish. Negative polarity of the tool is called direct polarity (d.p. in figure 5.3) and it has faster metal errosion rate.

Machining current I [A] Electrical current between the electrode and the workpiece during EDM pulse. Higher current means faster material removal.

Pulse on time T_{on} $[\mu s]$ Duration of the electrical pulse. Longer pulse means faster material removal.

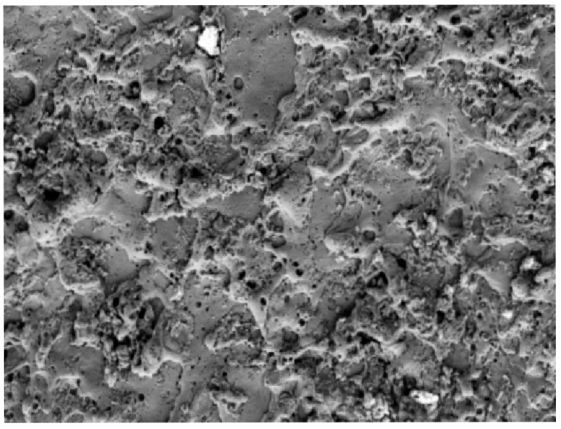

Figure 5.1: SEM micrograph of AISI 4140 steel under EDM conditions: $I = 1.5$ A and $T_{on} = 3.2$ μs [12]

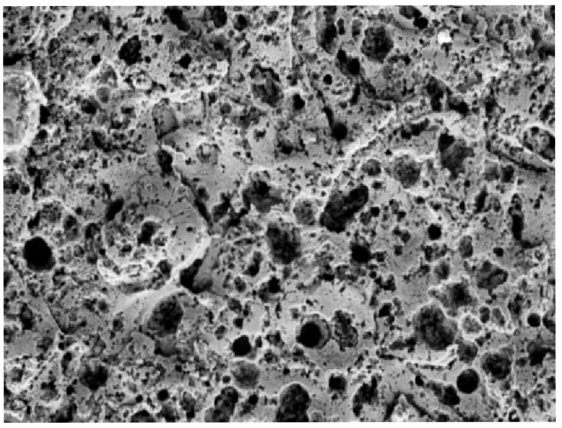

Figure 5.2: SEM micrograph of AISI 4140 steel under EDM conditions: $I = 12.5$ A and $T_{on} = 12$ μs [12]

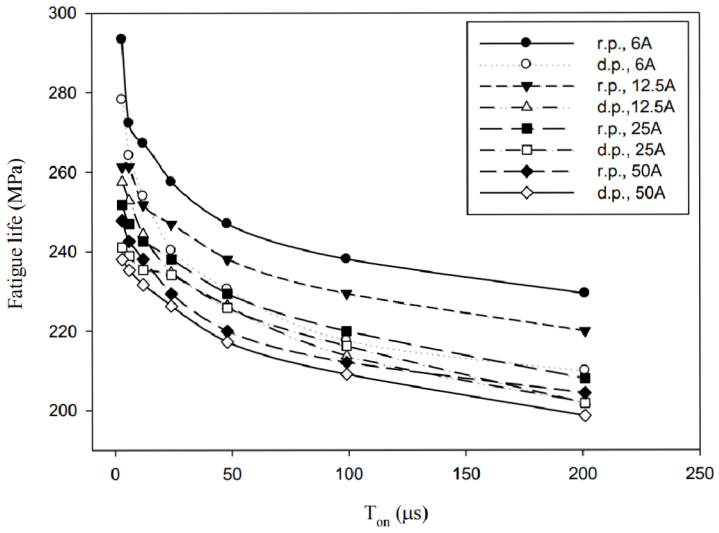

Figure 5.3: Fatigue limit of high manganese steel estimated by $\sqrt{}$ area method depending on tool polarity, T_{on} and I [13]

5.5. Effect of heat treatment and coating

It is known that compressive residual stresses at surface have positive effect on fatigue performance while tensile residual stresses at surface have negative effect. From figure 5.4 it is obvious that EDM causes tensile stresses at machined part surface. Tempering the tool after machining could relieve residual stresses in the tool and therefore improve its fatigue performance.

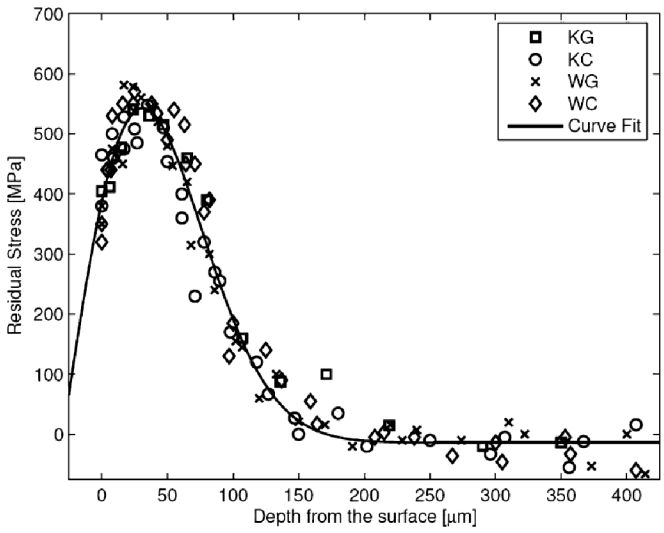

Figure 5.4: Residual stress distribution of 1.2738 DIN steel vs depth from the surface. KG – kerosene dielectric and graphite electrode, KC – kerosene dielectric and copper electrode, WG – water dielectric and graphite electrode, WC – water dielectric and copper electrode. [14]

6. 1857138 Mold analysis

Product manufactured in this mold is a 10 position connector housing for MQS and AMP Multiple Contact Point connectors (figure 6.1). The 2 problematic cores are forming secondary locks for MQS connectors.

The tool has 4 cavities, which means that 4 products are molded during 1 stroke of the injection molding machine. Polymer melt is transferred to each cavity through hot runner system. Both the injection half and ejection half have their own cooling circuit consisting of drilled holes connected with pipes and hoses. Pressure sensor (Kistler 6183A) is installed in each cavity, located near the last spot that is filled with polymer during the cycle to detect NOK parts and scrap them. Three-axis manipulator is removing the finished products from the mold.

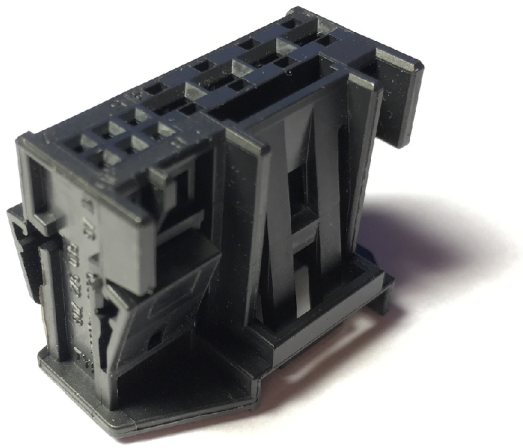

Figure 6.1: 10 position mixed housing

6.1. Mold material and manufacturing technology

Frame of the mold and most of the cores are made out of 1.2343 ESU steel. Some of the cores are made out of 1.2344 ESU steel and the thinnest ones including cores 531 and 532 are made out of powder metallurgical cold work tool steel Vanadis 4 Extra. There were some mechanical properties measured in compression (figure 6.2) and in bending (figure 6.3) in the material supplier data sheet, but a tensile test was performed to get full stress-strain curve of the material.

6.1.1. Tensile test

Three flat specimens with the thin cross section of 2 mm^2 were manufactured by EDM at the company's tool shop. It should be noted, that the specimen design is not following any tensile test specification. It was chosen to make the test possible on a testing machine with a force limit of 20 kN, even if the ultimate tensile strength would be the same as bend strength from figure 6.3. Because of the hardness of this material, at first all of the specimens were slipping from the tensile machine wedge grips at force around 3 kN. Therefore the design had to be modified - fixture device from softer steel was added

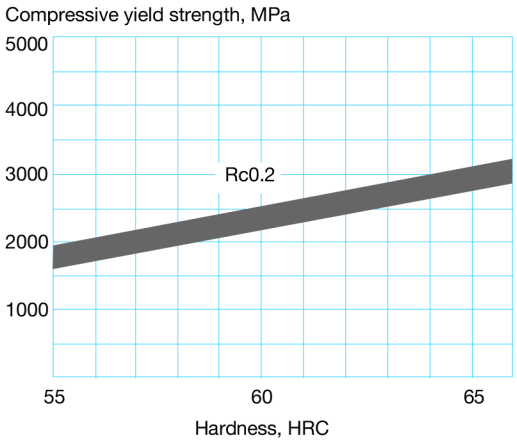

Figure 6.2: Compressive yield stress vs HRC hardness for Vanadis 4 Extra [15]

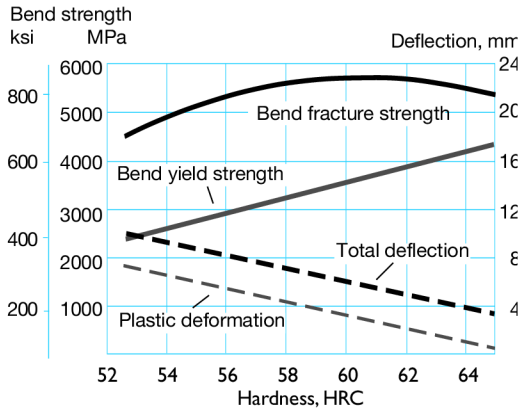

Figure 6.3: Four-point bend testing fracture strength, yield strength, total deflection and plastic deformation vs HRC hardness for Vanadis 4 Extra [15]

between the wedge grips and specimen. This fixture was then transfering the force to the specimen not just by friction but also by hardened steel pins fitting in cuts added to the specimen (figure 6.4).

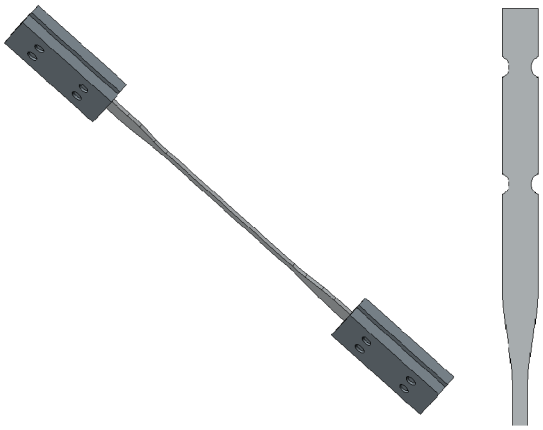

Figure 6.4: Specimen CAD design assembled with the fixture parts

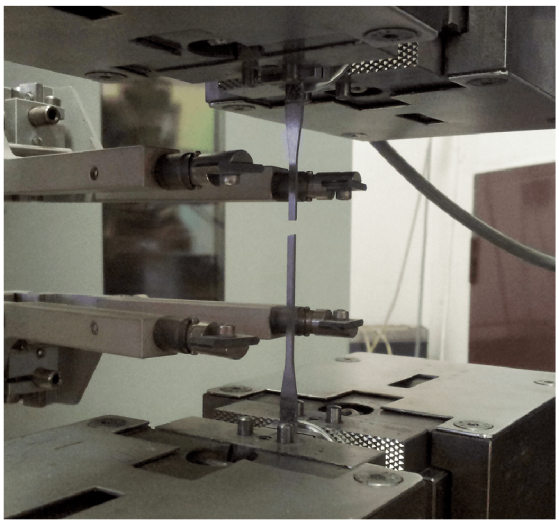

Figure 6.5: Tensile test setup

Table 6.1: Results of tensile test of Vanadis 4 Extra

Specimen No.	1	2	3	Mean
E [MPa]	218 306	219 511	219 703	219 174
$R_{p0.1}$ [MPa]	2010	1931	1961	1967
$R_{p0.2}$ [MPa]	2135	2097	2106	2113
R_m [MPa]	2444	2440	2441	2442
ε_f [–]	0.036	0.035	0.036	0.035

The test was performed at Brno University of Technology, Institute of Solid Mechanics, Mechatronics and Biomechanics on a ZWICK Z020 machine. The results can be seen in

table 6.1. Tensile yield stress for 0.2 % plastic strain was slightly higher than compressive yield stress for 0.2 % plastic strain from material data sheet. Ultimate tensile strength was less than 50 % of bend fracture strength listed in data sheet. Young's modulus was determined by secant between force values of 200 N and 2000 N.

6.1.2. Manufacturing technology of cores 531 and 532

Cores 531 and 532 are cut with EDM out of Vanadis 4 Extra steel block quenched to 54-56 HRC. There is no information available about machining current or pulse on time used for the process. The toolmakers only choose the number of cuts for each surface – higher number of cuts means better accuracy and surface quality, because smaller machining current and pulse on time is used. Number of cuts is chosen depending on each surface roughness defined in the tool drawing. There is no further heat treatment provided after machining.

6.2. Injection molding process simulation

Two commercial softwares were used for simulation of the injection molding process – Moldflow and Moldex3D. A simplified finite element model of the whole mold was created in both to capture the influence of mold heating up during production. The pressure results at pressure sensor location from each simulation were compared with actual pressure data from the sensor to validate the simulation. The mold produces 2 dash variants of the housing and is being run on 6 different injection molding machines, depending on the workload of each machine. There is a separate process sheet for each machine and on some machines there are different parameters for different product variant. However, the crucial parameters such as melt and mold temperature, injection speed, velocity/pressure switch-over or packing pressure are the same for all machines and variants. Parameters for machine KPL224 (Sumitomo Shi Demag Intelect 100-180) on which the mold runs most of the time were picked.

Table 6.2: Process parameters for 1857138 mold on machine KPL224

Parameter	Value
Polymer material	Ultradur B4300 G2 High Speed
Melt temperature [°C]	260
Mold temperature [°C]	60
Machine screw diameter [mm]	25
Shot size [mm]	46.86
Injection speed [$cm^3 \cdot s^{-1}$]	40
Velocity/pressure switch-over [mm]	8.96
Packing pressure 1 (0 – 0,3 s) [bar]	800
Packing pressure 2 (3,3 – 3,5 s) [bar]	500
Cooling circuits water temperature [°C]	60
Cooling circuits flow rate [$cm^3 \cdot s^{-1}$]	133.33
Mold-open time [s]	5.25

Material of the mold and cores had to be assigned (thermal conductivity and specific heat capacity) for heat transfer calculation. Additional thermal contact resistances between various parts of the mold were not taken into account.

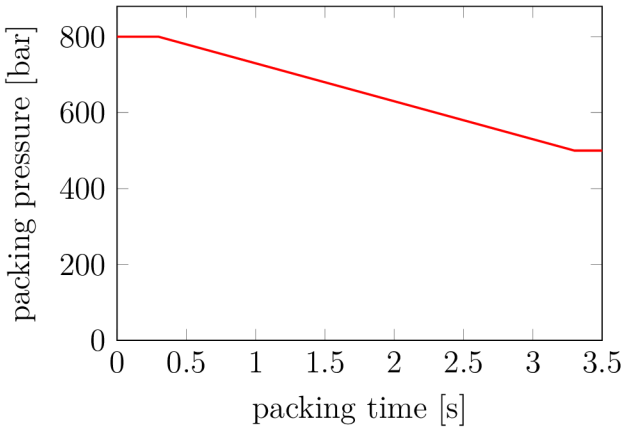

Figure 6.6: Packing pressure control for 1857138 mold

6.2.1. Moldflow

Moldflow supports all types of analysis methods from subsection 3.2.2. Dual domain method was chosen for this analysis due to thin-walled part geometry and hardware limitation for generating 3D mesh in Moldflow. As can be seen in figure 6.7, 1/4 symmetry was defined by occurence numbers on part and runner meshes. Sprues, runners and cooling channels were meshed with beam elements. The whole mold including cores 531 and 532 was simplified as one block of steel and meshed with tetrahedral elements (figure 6.9). It is also visible from this figure that there are many distorted elements in the mold mesh which is a weakness of Moldflow's meshing and could cause the results to be inaccurate.

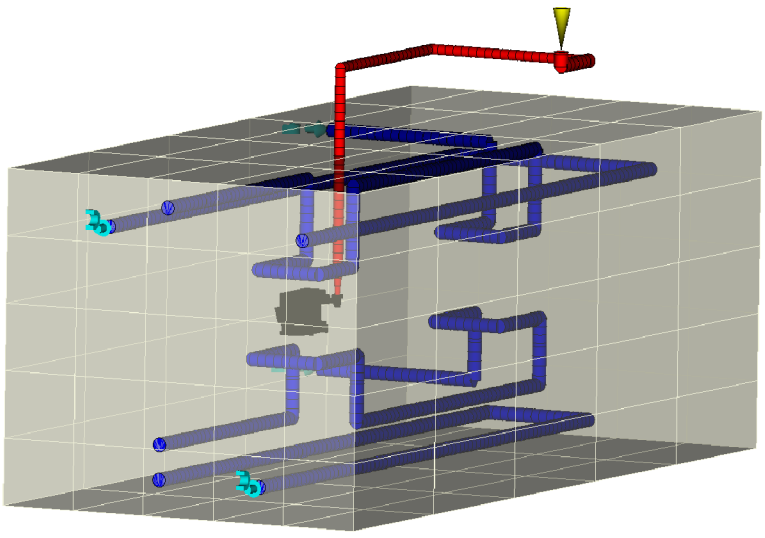

Figure 6.7: Model of the mold in Moldflow

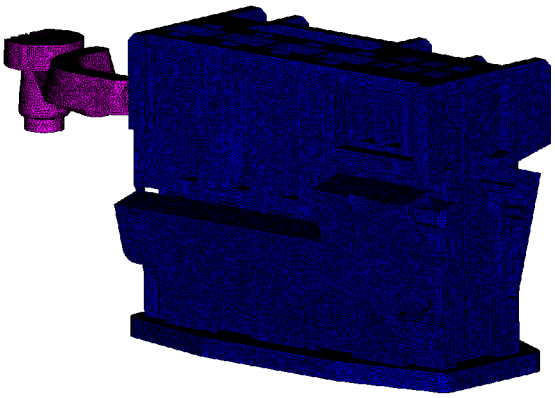

Figure 6.8: Mesh sizing for part

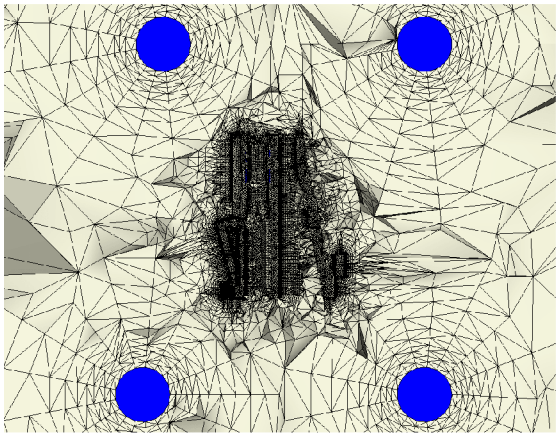

Figure 6.9: Mesh section showing meshes of part, cooling channels and mold steel

Mesh sizing on part was set to 0.25 mm (figure 6.8). There were 204 511 nodes on the part only and 11 656 676 elements on the whole mesh.

All the important material data was provided to Moldflow database by the polymer manufacturer.

6.2.2. Moldex3D

Moldex3D software only supports 3D analysis. The main difference from Moldflow is that it uses boundary layers through part thickness and generates automatic hexahedral meshes for sprues, runners and cooling channels defined by lines. Only 1/2 symmetry could be used in this software due to shape of the runner system and placement of the cavities inside the mold (figure 6.10).

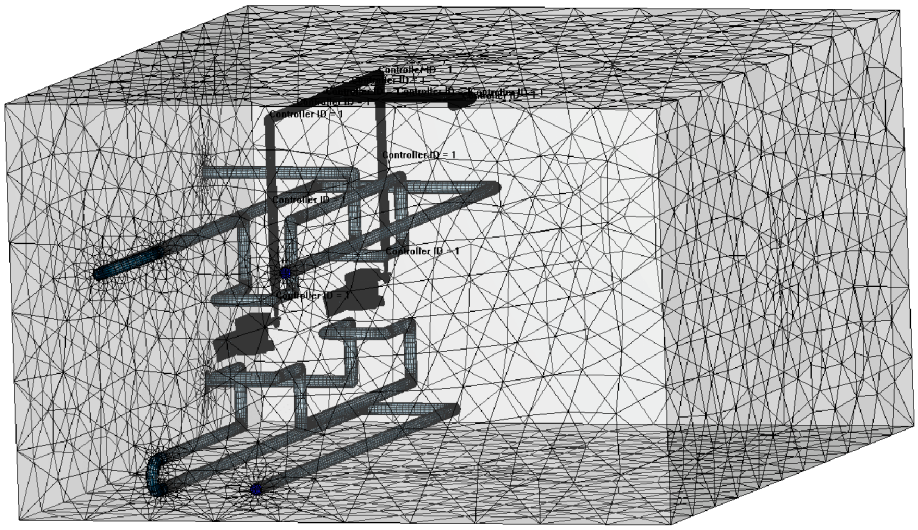

Figure 6.10: Model of the mold in Moldex3D

The part and its cold runner were merged. Cores 531 and 532 were also imported and defined as mold inserts. The rest of the mold was again simplified as one block of steel. Mesh sizing on part was set to 0,5 mm and refined to 0,25 mm near contact areas with

the cores. All the common surfaces on part and cores had to be split to enable matched surface meshes. There were 1 701 898 nodes and 5 649 836 elements on the complete mesh.

All the important material data was provided to Moldex3D database by the polymer manufacturer.

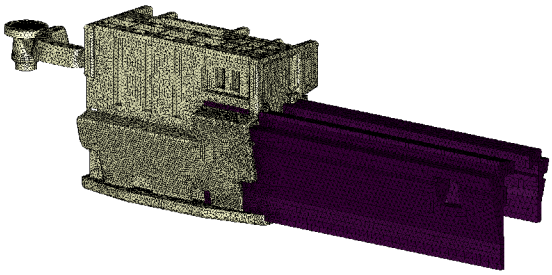

Figure 6.11: Mesh sizing for part and mold inserts

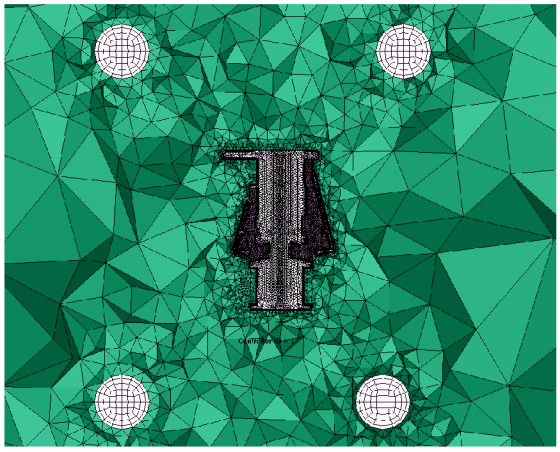

Figure 6.12: Mesh section showing meshes of part, mold inserts 531 and 532, cooling channels and mold steel

Three analyses were ran to see how close could the pressure results at sensor location get to the pressure data from production for each approach.

Filling, packing (F, P) This is the simplest type of analysis. It assumes that the mold wall has uniform temperature and does not heat up at all during production. It is generally used in early stages of mold design to predict the filling pattern and some weaknesses in part design that could complicate its production. It only uses the mesh of the part and runners, requiring much less preprocessing time. For molds that have an effective cooling system the pressure results can be sufficiently accurate.

Transient cooling, filling, packing (CT, F, P) This analysis takes the cooling system of the mold into account. First, a transient cooling analysis is run repeatedly. The amount of heat introduced to the mold by polymer melt is being taken away through mold walls and cooling channels during the cycle. When the mold temperature difference between following cycles drops below certain value, a steady-state mold temperature profile is reached. This temperature profile is then used in filling and packing analysis. This analysis predicts heat accumulation on the mold and its inserts and how it affects the polymer melt flow. It can be used to predict cooling times and cooling system efficiency.

Transient cooling, filling, packing with reduced injection speed It is common for older injection molding machines that the screw head gets worn out and backflow of polymer during filling occurs. This means that the actual injection speed is a little smaller than the one set on the injection molding machine, which the simulation normally does not take into account. To imitate this behavior, one analysis with injection speed reduced from 40 $cm^3 \cdot s^{-1}$ to 35 $cm^3 \cdot s^{-1}$ was made.

6.2.3. Results validation

Results of pressure at sensor location during injection molding cycle can be seen at figure 6.15. Curves from Moldex3D are much smoother than the one from Moldflow because Moldex3D allows the user to define a sensor node (at pressure sensor location) at which all flow analysis time steps will be saved.

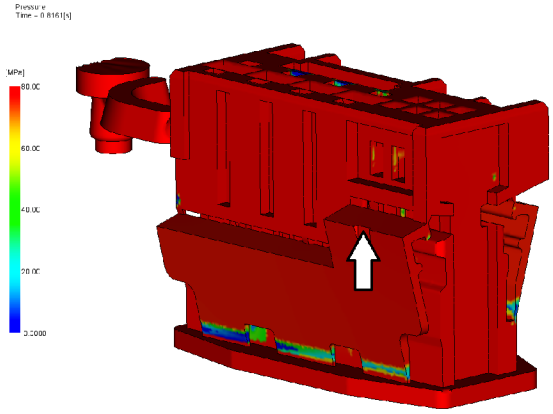

Figure 6.13: Pressure distribution on the part predicted in Moldflow during peak pressure ($t \approx 0.8$ s) at sensor location (white arrow)

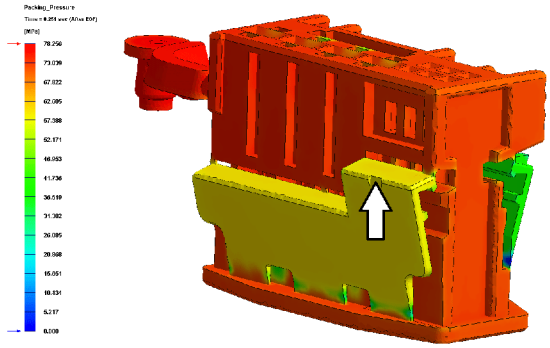

Figure 6.14: Pressure distribution on the part predicted in Moldex3D during peak pressure ($t \approx 0.8$ s) at sensor location (white arrow)

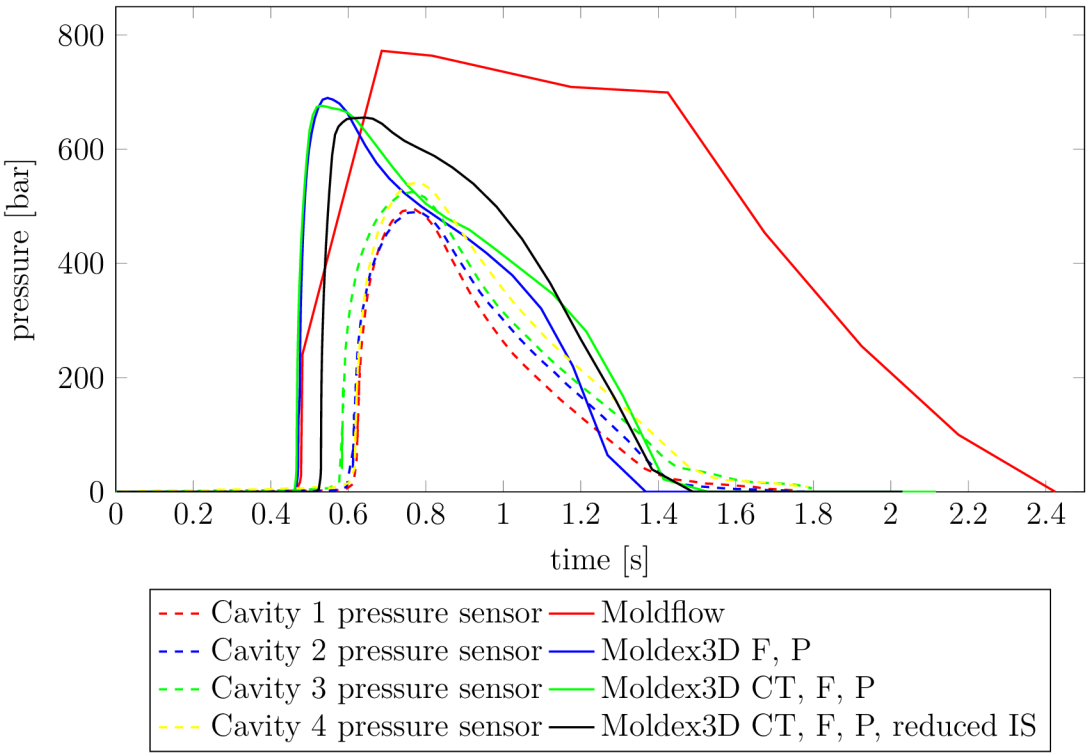

Figure 6.15: Comparison of pressure results at sensor location from various simulations with pressure sensor data, Moldex3D CT, F, P, reduced IS (black curve) was chosen as an input for the structural simulation

Simulation in Moldflow predicted a pressure peak much higher than the one measured by pressure sensor and also much slower cooling and solidification of the polymer. This may have been caused by poor mesh quality (figure 6.9). The curve that was closest to pressure sensor data and therefore most accurate was from Moldex3D simulation of transient cooling, filling and packing with reduced injection speed.

Another interesting founding was, that according to the simulation, the current velocity/pressure switch-over (at 8.96 mm screw position) would occur after 100 % of the cavity is filled. This process condition should never occur, because it means, that the piston is still forcing more polymer to the already filled cavity (normally the V/P switch-over occurs when 90-98 % of cavity is filled). This means high clamping force and usually damage to the tool. Based on the simulation results, the V/P switchover position should be set somewhere around 10.8 mm, when 98 % of the cavity is filled. However, because the simulation is not totally accurate (it was stated above that it often tends to fill the cavity much faster than the real machine due to machine imperfections), in reality the switch-over can happen when less than 100 % of the cavity is filled and this founding could have no real significance.

It is possible to export pressure and temperature profiles to a .cdb mesh created in Ansys using FEA interface in Moldex3D. The output is a .cdb file for each load step including the whole mesh and a set of SFE commands for pressure or BF commands for structural temperature loads. To use these files in Ansys Workbench, they had to be processed by a script in Matlab that only keeps the SFE and BF commands and deletes the rest of the file. Then they could have been input as load steps via command line feature in Ansys Workbench.

6.3. Structural simulation

In [3] it was stated that these types of simulation can be performed as static due to high damping effect of the polymer.

For the structural simulation, simplified parts of surrounding cores had to be added to model of geometry (figure 6.16), because they are in contact with cores 531 and 532 and affect their stress field. Contacts where in reality no separation could occur were defined as bonded. Other contacts were defined as frictionless. Mesh dense enough to capture the overall stiffness was created (figure 6.17). Outer walls of the surrounding parts were set as fixed.

To get accurate stress and strain results, submodels of areas near crack initiation were created and loaded with displacements (in load case that includes temperature also with temperatures) from the main model. These submodels were not loaded with any pressure profiles. This was tested to not change the results significantly and moreover, having to export pressure profiles again for each submodel would take a lot more preprocessing time. Contacts in these submodels were also defined as frictionless. Very dense mesh was created in the areas of stress and strain observation.

6.3.1. Models of material

Linear elastic models for the surrounding cores materials were created out of data sheets. Multilinear model with isotropic hardening of Vanadis 4 Extra was created from tensile

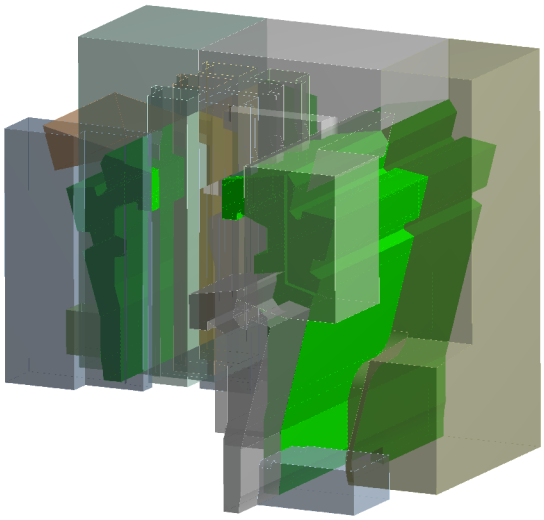

Figure 6.16: Model of geometry for structural analysis

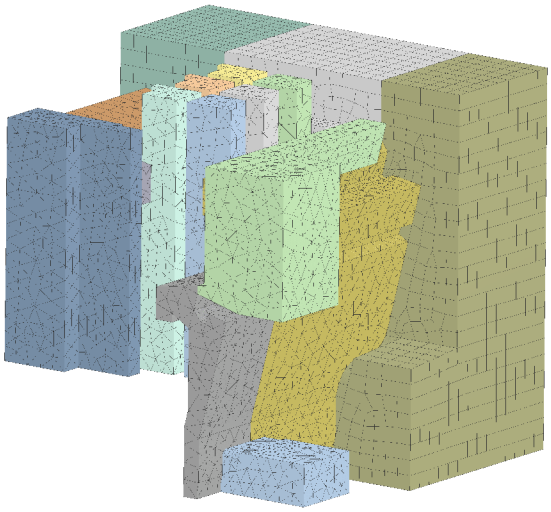

Figure 6.17: Mesh for structural analysis of the main model

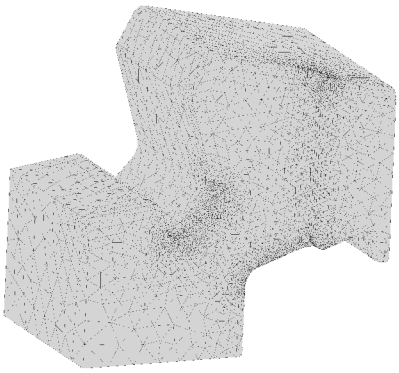

Figure 6.18: Mesh on submodel of core 532

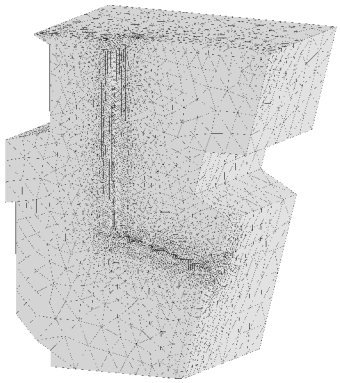

Figure 6.19: Mesh on submodel of core 531

test data (figure 6.20). A linear elastic model was also created from the same data to validate the accuracy of Neuber rule used in Ansys fatigue toolbox.

6.3.2. Applying pressure and temperature results to structural simulation

The process of one-way coupled analysis to analyze core stress due to uneven polymer melt is not so straightforward. When the polymer starts to solidify at some location, the pressure there drops drastically. As the solidification first occurs during packing and near the outer walls of the mold cavity, there usually are time steps with packing pressure acting on one side of the core and zero pressure on the other side where the polymer is already solidified. Using this uneven pressure profile as an input for structural simulation causes extremely high mechanical stress on the core.

In reality, solidified polymer is present at these locations and can be potentially acting as a support against the pressure on the other side of the core. To assess the influence of this effect, a simplified simulation only with linear model of material was carried out. Core 531 was left out in this simulation. Two cases were examined:

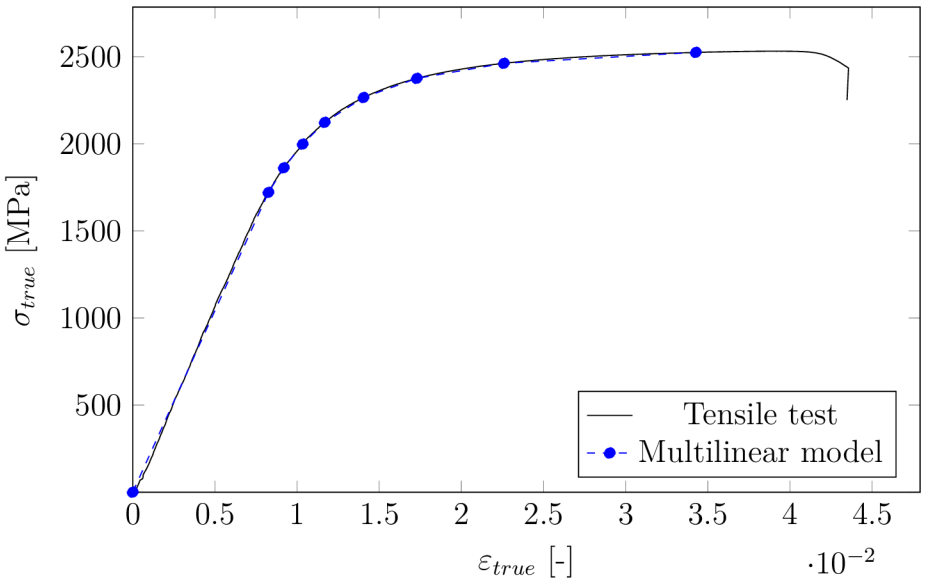

Figure 6.20: Multilinear model of material created from tensile test data

1. Surfaces on one side of the core were loaded with pressure of 70 MPa (packing pressure is changing from 80 to 50 MPa). The other side of the core was left free, therefore this would be the case when pressure profiles from packing after partial polymer solidification would be used as inputs for the structural simulation.

2. The same surfaces were again loaded with 70 MPa, but another body was added to the model to represent the solidified polymer on the other side of core 532. The average temperature across thickness of the polymer right after solidification is, according to simulation results, around 200 °C. Tensile modulus of the polymer body was therefore set for this temperature according to figure 6.21 (745 MPa). Frictionless contact was defined between the polymer body and core 532.

As can be seen in pictures 6.22, 6.23, 6.24 and 6.25, adding the solid polymer to the model changed the results significantly. This proves that if we want to do one-way coupled analysis also during packing, the effect of solid polymer supporting the tool should be somehow taken into account. Unfortunately this is out of reach of this master's thesis for following reasons:

- The size of the solidified region is changing for every time step.
- The temperature and therefore tensile modulus and stiffness of the solidified region is changing for every time step.
- As the polymer cools down, it shrinks and gap can be created between the tool and the polymer.
- As said in [4], describing the solidification especially of semi-crystaline polymers in simulation accurately is still a big challenge for current commercial codes. In other words it is still difficult to predict what exactly is happening in the mold during polymer solidification.

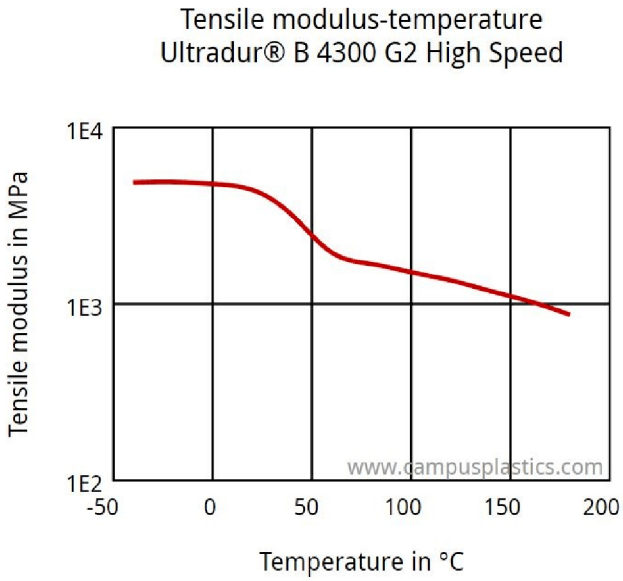

Figure 6.21: Plot of tensile modulus vs temperature for Ultradur B4300 G2 High Speed [17]

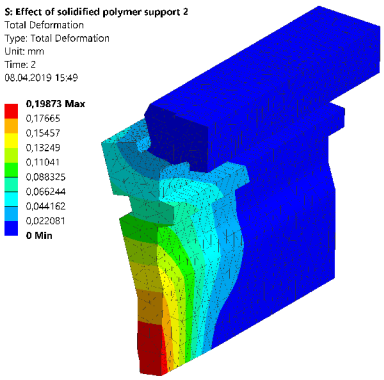

Figure 6.22: Total deformation results for case 1 (no polymer supporting core 532)

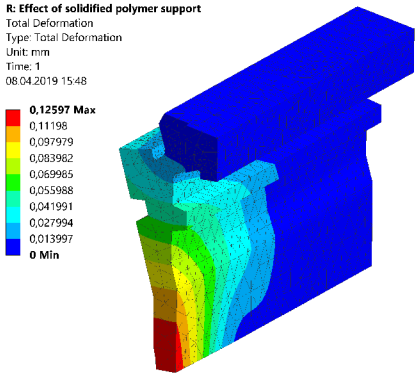

Figure 6.23: Total deformation results for case 2 (polymer supporting core 532)

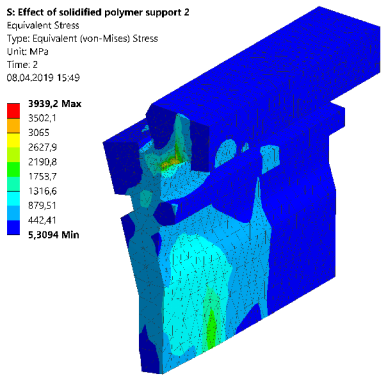

Figure 6.24: Equivalent stress results for case 1 (no polymer supporting core 532)

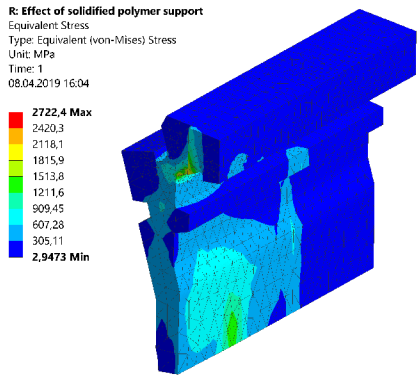

Figure 6.25: Equivalent stress results for case 2 (polymer supporting core 532)

For the reasons mentioned above, pressure profiles only up to a point of polymer solidification and significant pressure drops in areas near the problematic cores were used as an input for the structural simulation. These were up to 0.589 s of the cycle.

6.3.3. Load cases

Three types of load cases were examined:

Pressure load (P) Pressure profiles from 13 Moldex3D injection molding time steps were mapped to mesh from figure 6.17.

Pressure and temperature load (P+T) Pressure and temperature profiles from 13 Moldex3D injection molding time steps were mapped. Thermal expansion of the cores was considered in this case.

Scaled pressure load (scaled P) It is obvious from plot 6.15 that even the most accurate injection molding simulation predicted pressure peak higher by roughly 110 bar than the actual pressure detected by sensor. To make the simulated pressure peak even with the measured one, all pressures were scaled by factor 0.826 in this load case.

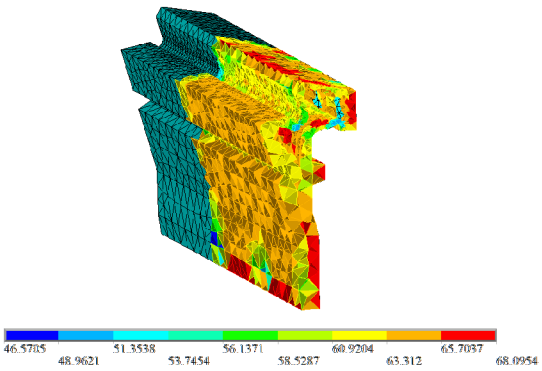

Figure 6.26: Pressures [MPa] from Moldex3D mapped to 532 core mesh

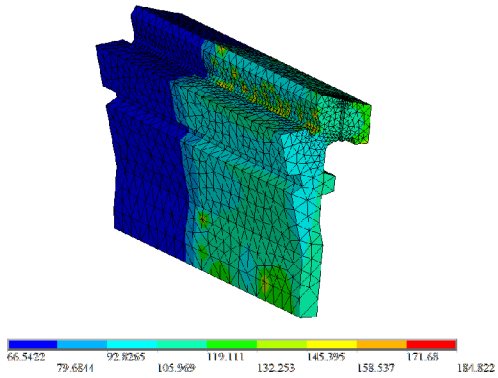

Figure 6.27: Temperatures [°C] from Moldex3D mapped to 532 core mesh

6.3.4. Results

The most important result from this analysis was the maximum equivalent total strain (ε_t) in the critical notch of each core (figures 6.28 and 6.29). This result is the main input to fatigue analysis (in form of amplitude $\varepsilon_a = \varepsilon_t/2$). Other important results were maximum values of equivalent stress, signed equivalent stress, maximum principal stress and absolute maximum principal stress in the same location where maximum equivalent total strain occurs. These are used in the Morrow modification of Manson-Coffin curve (equation 5.6) in form of mean stress $\sigma_{mean} = \sigma_{max}/2$.

Biggest strain values were obtained out of pressure and temperature load (P+T), in fact, the strain was more than 3 times bigger than other load cases. This means that much lower numbers of cycles will be obtained for this load case. The location of maximum

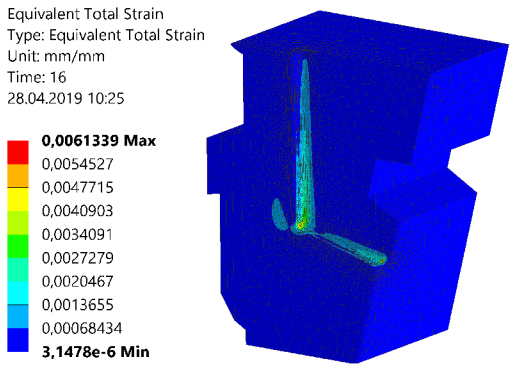

Figure 6.28: Maximum equivalent total strain on core 531 ($t \approx 0.52$)

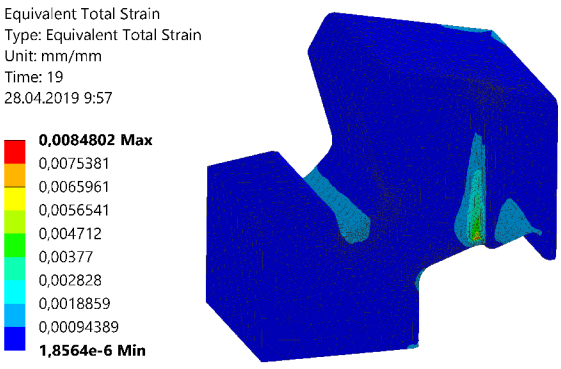

Figure 6.29: Maximum equivalent total strain on core 532 ($t \approx 0.59$)

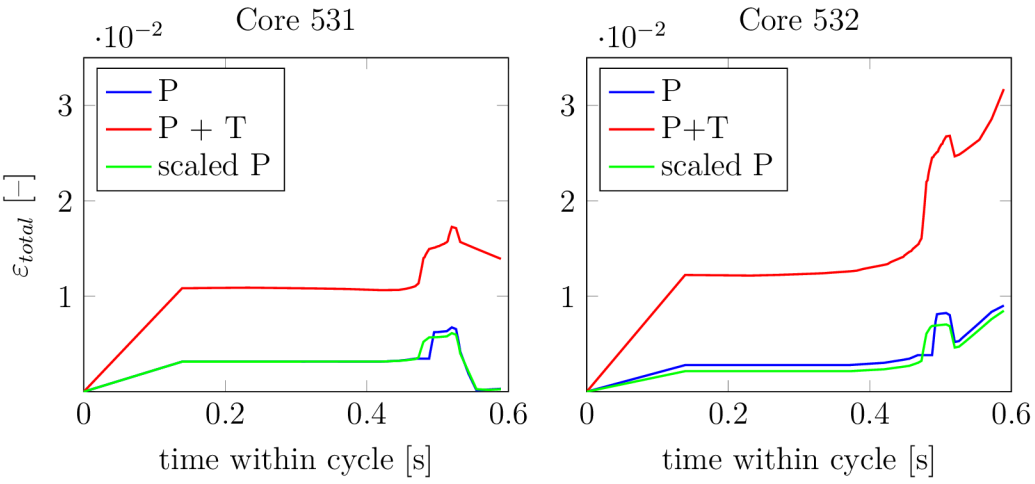

Figure 6.30: Maximum equivalent total strain on the cores during mold filling

Table 6.3: Results of structural simulation of the current state of core 531

Load case	Multilinear model		Linear model	m [–]
	Equivalent plastic strain [–]	Equivalent total strain [–]	Fictional stress [MPa]	
P	0	0.00674	–	–
P+T	0.00653	0.01728	3491	0.17
Scaled P	0	0,00613	–	–

strain on core 532 was matching with the actual fatigue crack position. For core 531 no such match was achieved (the maximum strain occured in different corner)

Values of m exponent that should normally lie in interval $(0, 1)$ were varying greatly between each load case and sometimes were even out of this interval. From that we can conclude, that Neuber rule is not applicable in this case. This may be caused by the fact that there is also contact pressure present in maximal strain area. Because of this, the problem had to be solved with the multilinear material model each time to determine fatigue lifetime.

Table 6.4: Results of structural simulation of the current state of core 532

Load case	Multilinear model		Linear model	m [–]
	Equivalent plastic strain [–]	Equivalent total strain [–]	Fictional stress [MPa]	
P	0.00049	0.00902	2000	-0.19
P+T	0.02028	0.03170	4797	0.36
Scaled P	0.00010	0.00848	1736	5.9

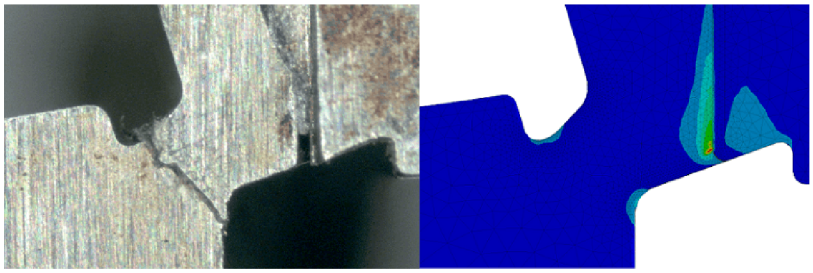

Figure 6.31: Maximum strain on core 532 matching actual fatigue crack position

6.4. Fatigue analysis

Due to plastic deformation inside critical notch of core 532 and therefore hard loading, Manson-Coffin strain-life curve was chosen to describe crack initiation. Both methods from table 5.1 were tried out to estimate its parameters. Only the universal slopes method by Manson was used in the end (plot 6.32), because negative values of ψ were coming out of the method by Bäumel and Seeger (this method is only valid for low-alloy steels).

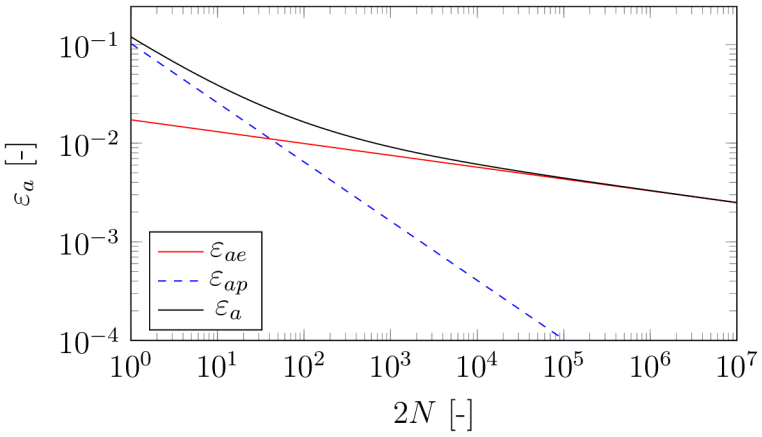

Figure 6.32: Manson-Coffin curve for Vanadis 4 Extra estimated by Universal Slopes Method from Manson

Morrow mean stress correction from equation 5.6 was used. On the drawing of the cores, no surface roughness is prescribed on the surfaces where the crack is initiated. They were assumed to be equal rougness to a grinded surface which, according to [11],

corresponds with a surface effect factor of 0.81. The σ'_f in equation 5.1 was multiplied by this factor. Different stress components at the location of maximum total strain were used to find out which one gives us results closest to the actual fatigue lifetime for current state. The latest information by production was that that core 532 lasts around 30 days of pure production which is about 170000 cycles for given cycle time and breakage on core 531 occurs much less frequently.

Table 6.5: Results of fatigue analysis for the current state of core 531, for various load cases and mean stress definitions

	Number of cycles till crack initiation ($2N$), different mean stress definitions			
Load case	Equivalent stress	Signed equivalent stress	Maximum principal stress	Absolute maximum principal stress
P	195 000	3 200 000	1 100 000	4 600 000
P+T	435	4750	1700	7600
Scaled P	4 700 000	6 000 000	2 350 000	8 800 000

Table 6.6: Results of fatigue analysis for the current state of core 532, for various load cases and mean stress definitions

	Number of cycles till crack initiation ($2N$), different mean stress definitions			
Load case	Equivalent stress	Signed equivalent stress	Maximum principal stress	Absolute maximum principal stress
P	15 000	420 000	100 000	561 000
P+T	60	225	150	345
Scaled P	24 000	660 000	165 000	950 000

The most accurate values were obtained from scaled pressure (scaled P) load case in combination with maximum principal stress component as mean stress. The pressure and temperature load (P+T) was giving unrealistically small numbers of cycles. The possible reasons for this will be discussed later in the conclusion of the thesis. Based on these results, the scaled pressure load was used to determine the influence of geometry change on fatigue lifetime.

6.5. Parameters modification

The only two parameters change analysed by simulation was geometry of the cores and V/P switch-over position. However, changes of other parameters will also be discussed and if possible, justified by using other sources.

6.5.1. Geometry change

Unfortunately, the injection mold is such a complex system that the changes of its geometry to prevent core breakage are very limited. The functionality of the mold and the molded product must be maintained. Sometimes, it is not possible to do some change, because the product design can not be changed in this way. Sometimes, it is not possible to make one core thicker and the other one thinner, because this means the breakage could just move to the other core.

The biggest possible radius for currently more problematic core 532 was 0.2 mm. Radius of 0.3 mm is also checked for core 531 in notch where the crack is visible on figure 2.3, even though the simulation predicted a different notch as critical.

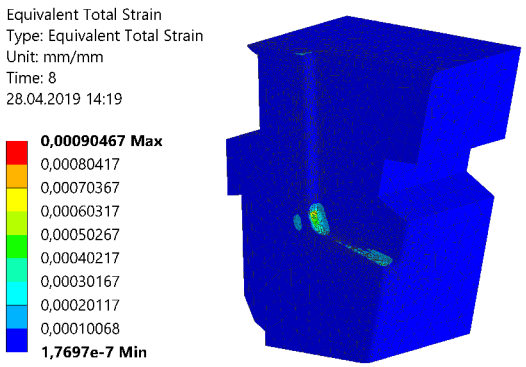

Figure 6.33: Maximum equivalent total strain on core 531 ($t \approx 0.52$)

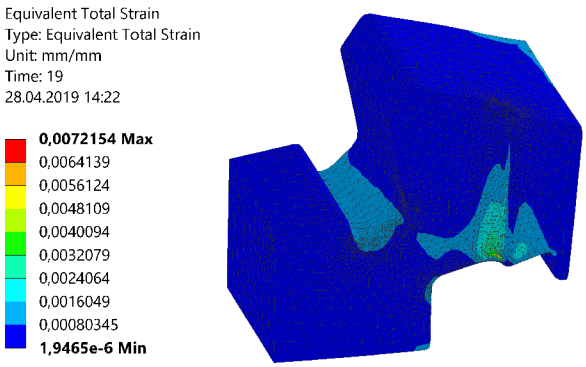

Figure 6.34: Maximum equivalent total strain on core 532 ($t \approx 0.59$)

As can be seen in figure 6.29, adding radius to core 532 could help to reduce equivalent total strain amplitude. Using the model from section 6.4, increase from 165 000 cycles to 1 850 000 cycles lifetime (from 30 days to more than 320 days) can be expected, therefore applying this design change is recommended. Adding radius to core 531 reduced the already low equivalent total strain amplitude and according to the fatigue model, would increase its lifetime from 2 350 000 to infinite lifetime, therefore this design change is also recommended.

6.5.2. Change of V/P switch-over

It was mentioned in subsection 6.2.3, that with current process settings, the simulation predicted the V/P switch-over to occur after 100 % of the cavity volume is filled (the simulation automatically switches to packing when 100 % of the cavity is filled). It was tested what will happen with the peak strains on the cores, if the V/P switch-over will occur earlier – when 90 % of the cavity is filled, which corresponds to a screw position of 14.5 mm instead of current 8.96 mm. This could relieve the pressure load on the cores, because the mold is not filled so quickly in this case.

The pressure profiles were also scaled by the same factor of 0.826 as in subsection 6.3.3 to make the simulated peak even with the measured peak (figure 6.35). From the simulation results it can be seen, that changing this process parameter will move the equivalent total strain peak on core 532 from 0.59 s to 0.506 s within cycle and only slightly reduce the maximum value. This change would extend the lifetime from 165 000 cycles

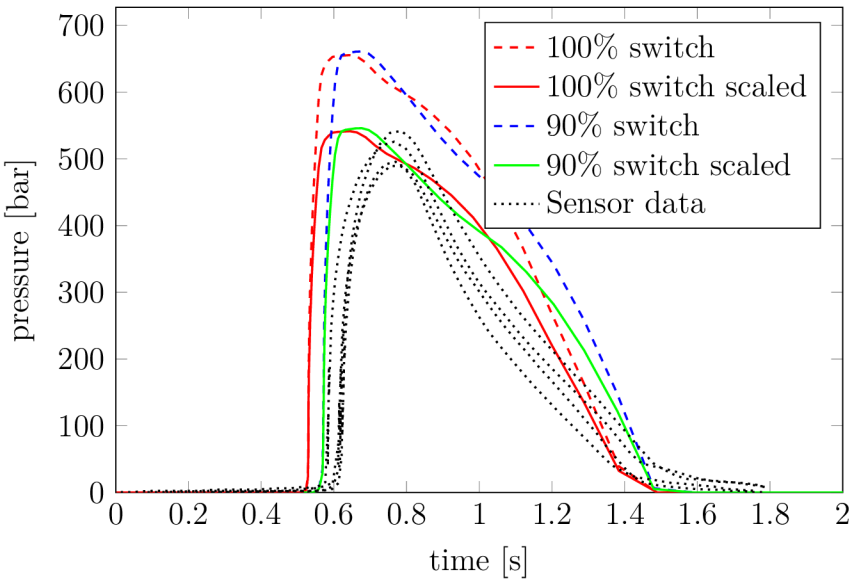

Figure 6.35: Comparison of pressure results at sensor location. Pressure profile with V/P switch-over at 100% (original and scaled) vs pressure profile for V/P switch-over at 90% (original and scaled)

to only 190 000 cycles, which is probably negligible considering fatigue data scatter. No difference in maximum strain was observed on core 531.

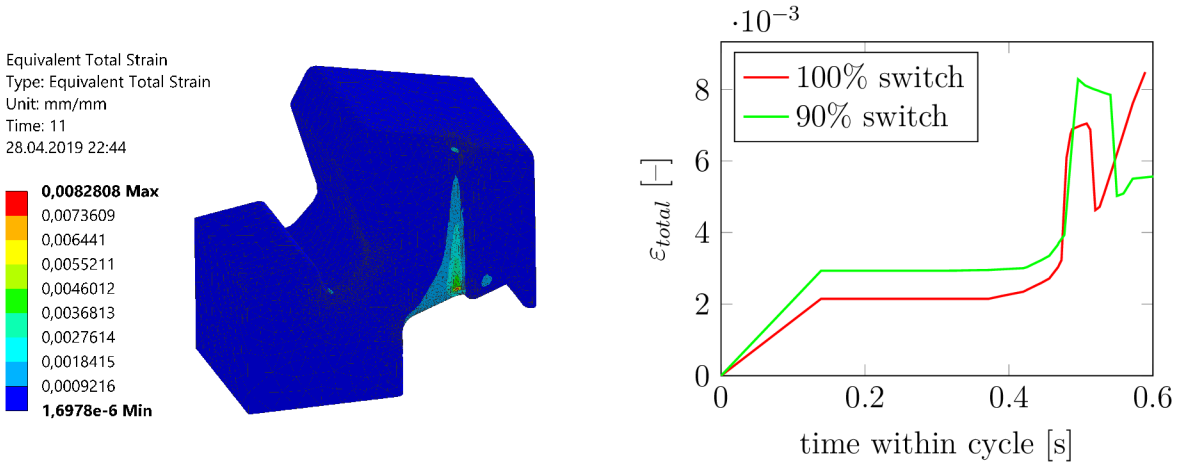

Figure 6.36: Comparison of strains on core 532 before and after changing the V/P switch-over

Based on the results above, this change of parameter is not recommended since it would enlarge cycle time which means higher production costs for almost no core fatigue lifetime extension.

6.5.3. Material change

Currently there is no material with higher strength available at the company. Vanadis 4 Extra was compared with various other materials for molding cores across more plants and came out as the best material for frequently breaking tools. 1.2344 ESU steel was

recommended by mold designer from Germany, but this material was already used in the past for the same cores with no better results. There is no tensile test data for 1.2344 ESU steel and the data in table 6.7 are from data sheet. 1.2344 ESU has ultimate tensile strength by 432 MPa smaller than Vanadis 4 Extra. This would most definitely also mean weaker fatigue performance.

Table 6.7: Comparison of mechanical properties of Vanadis 4 Extra and 1.2344 ESU steels

Mechanical property	Vanadis 4 Extra	1.2344 ESU
E [GPa]	219	215
$R_{p0.1}$ [MPa]	1967	–
$R_{p0.2}$ [MPa]	2113	–
R_m [MPa]	2442	2010

6.5.4. Manufacturing technology change

In the tool drawing, there is no surface roughness defined for surfaces where the fatigue cracks are initiated, simply because they do not form any surfaces on the molded product. This means they are probably machined by small number of cuts. Horizontal scratches can be seen on figure 2.3 and vertical scratches on figure 2.4 (both pictures taken by optical microscope). As explained in subsection 5.4, if these surfaces were finished as smooth as the other surfaces, it could extend the tool fatigue lifetime.

6.5.5. Heat treatment

It was shown in 5.5 that EDM machining causes residual tensile stresses. In [15] the tool material supplier reccomends a stress relieving heat treatment procedure after rough machining. Heating the tool up to 650°C, holding time 2 hours, cooling slowly to 500°C and than freely in air. This procedure should be applied to all cores from Vanadis 4 Extra that have breakage issues.

7. Conclusion

Two commercial injection molding simulation softwares were compared – Moldflow and Moldex3D. The only advantage of Moldflow was much more comprehensive help database and user forums, which made it easier to look for solutions to problems with operating this program. The main advantage of Moldex3D was much easier and faster preprocessing with using the same hardware. The boundary layer mesh generated from Moldex3D is much more suitable for injection molding simulation, had overall better element quality and was done using less effort and hardware time. The disadvantage of Moldex3D is that if we want to export the moldbase pressure profiles, we need a fully matched mesh between part and moldbase (meaning that every node on the common surface is the same for the part and the moldbase). Making a fully matched mesh for geometrically complex parts can add a lot of preprocessing time, since it requires manual splitting of all common surfaces. The resulting pressures from Moldex3D were much closer to those measured by pressure sensor in the cavity, but still about 20% higher.

It was also observed that these types of simulation tend to fill the cavity faster, than the real machine. This can be caused by worn out screw head on the machine and resulting backflow of polymer. This effect was partially evened out by using injection speed of 35 $\mathrm{cm}^3 \cdot \mathrm{s}^{-1}$ instead of the 40 $\mathrm{cm}^3 \cdot \mathrm{s}^{-1}$ from process sheet.

If the mold is cooled well, there is no need to also run transient cooling analysis to obtain accurate pressure profiles. A simple filling and packing analysis is much easier for preprocessing and the pressure profiles from it are almost identical to transient cooling, filling and packing analysis (the difference between the green and blue curve on figure 6.15, which takes much more preprocessing time. If the user still wants to check the influence of mold overheating, the easiest and most accurate way would be to measure the actual cavity temperatures on moldbases and cores during the production and enter them to the simulation directly.

Using submodels to investigate the strain peaks on different parts of the cores is very helpful in this case. It allows us to have the main model with much less elements and makes the pressure export from Moldex3D faster. These submodels do not need to be loaded with pressures as well, as long as they are small enough compared to the main model.

Another finding was, that using pressure profiles from time steps when the polymer starts to solidify and the pressure there drops significantly (during packing), is disputable. On a simplified model it was shown, that when the polymer on one side of the core solidifies and the other side of the core is still under pressure of the melt, the effect of solid polymer supporting the core has not negligible effect on the core deformation and stress. Because the interaction between polymer and tool during packing can be unpredictable and no research was found on this topic, only the time steps until 0.59 s of the cycle (before solidification near the cores) were used as boundary conditions in the structural simulation.

Peak stresses and strains on core 531 occured just before the mold cavity was filled ($t \approx 0.52$). For core 532 it was right after the cavity was filled ($t \approx 0.59$).

The method chosen to describe the fatigue life was Manson-Coffin curve estimated from tensile test data by universal slopes method. The effect of non-zero mean stress was taken into account using Morrow mean stress theory with maximum principal stress. The effect of imperfect surface was included in surface effect factor of 0.81. The Neuber rule

was found to be inapplicable in this case which may have been caused by contact pressure present in maximum strain areas. The input to Manson-Coffin curve was equivalent total strain from non-linear solution.

Including thermal expansion in the structural analysis caused high strain increase which led to extremely small fatigue predictions. The first reason for this could be not including the mold clearances in the model. Some clearances are always present in the mold for venting purposes (the air is being pushed out of the cavity by polymer melt and it must get out somehow) and it is possible that the thermal expansion would in reality only reduce or close those clearances. The other reason may be inaccurate determination of heat transfer coefficient (HTC) between the melt and mold walls. The option "Automatically determined HTC" was chosen in Moldex3D, but there is no detailed explanation in the software manual on how this automatic determination works. Higher HTC means higher heat flux into mold walls and therefore smaller temperatures of polymer calculated. Because the polymer viscosity is also a function of temperature, this can lead to overestimated injection pressure prediction, which corresponds with the fact that the simulated pressure peak was always 20 % higher than the measured one. This higher heat flux would also mean overestimated tool temperature predictions. Unfortunately there is no temperature sensor installed in the analysed tool cavity and no measurements of tool temperature during production (usually done with a contact thermometer) were available, which means there was no way to verify or disprove the calculated tool temperatures. For these reasons, the thermal expansion was not used for parameters change validations. The most accurate numbers of cycles were obtained from pressure profiles scaled by factor of 0.826 to make the simulated pressure peak even with the peak measured by pressure sensor. This approach was then used to validate parameters change suggestions.

It was found that adding radius of 0.2 mm to the critical notch on core 532 could increase its fatigue lifetime from 30 days to more than 320 days of production. Since the manufacturing cost of this core is 240 EUR and the tool has 4 cavities, this design change would bring up to 10 600 EUR of savings every year (depending on how often will the mold produce). If this design change proves to be successful, it could be applied to other molds with similar cores. Adding radius of 0.3 mm to the notch on core 531, where breakage occurs, would further reduce the strain amplitude and could prolong its lifetime to infinite life, which means additional savings.

Last parameter tested by simulation was the process parameter V/P switchover position. When moving the switchover from 100% cavity filled to only 90% cavity filled (and also scaling the pressure profiles by the same factor of 0.826), it caused only a small drop of maximum equivalent strain. This drop would extend the lifetime from 165 000 to only 190 000, which is negligible and therefore changing this parameter was not proposed.

To sum up, it is not always necessary to do an FSI analysis in order to extend injection molding core fatigue lifetime. This analysis is fairly complicated, takes a lot of effort and the results are often not worth the time spent on this analysis. When a frequent breakage occurs on any core, these procedures are generally recommended:

1. Find the locations where the cracks are initiated from. Specifically look for sharp corners and notches. Than make these notches as round as possible. Unfortunately this is often limited by the existing product and mold design.

2. Focus on the manufacturing process of the tool (EDM in case of this thesis). If the surface on the tool is not forming any surface on the molded product, it is usually

machined using only one cut which leads to bigger surface roughness. If the cracks are formed from this surface, using more cuts for this surface should be considered.

3. Consider adding heat treatment process after machining. The heat treatment should be only to remove the residual stresses from previous machining and should be according to instructions of the material supplier.

4. Adding protective coating could also help in some cases.

5. Changing the injection molding process parameters such as reducing injection speed, moving the V/P switchover to smaller % of cavity volume filled or reducing packing pressure can be considered. On the other hand it must be kept in mind that any change of process parameters can introduce defects on the product, therefore the parameters changes must be tried out on the actual machine and the final parts must be inspected for those defects.

Bibliography

[1] CARPENTER, Brian, PATIL, Sachin, HOFFMAN, Rebecca, LILLY, Blaine and CASTRO, Jose, 2006, Effect of machine compliance on mold deflection during injection and packing of thermoplastic parts. *Polymer Engineering & Science* [online]. 2006. Vol. 46, no. 7p. 844-852. [Accessed 18 April 2018]. DOI 10.1002/pen.20527. Retrieved from: http://doi.wiley.com/10.1002/pen.20527

[2] AHN, Dong-Gyu, KIM, Dae-Won and YOON, Yeol-Ui, 2010, Optimal injection molding conditions considering the core shift for a plastic battery case with thin and deep walls. *Journal of Mechanical Science and Technology* [online]. 2010. Vol. 24, no. 1p. 145-148. [Accessed 18 April 2018]. DOI 10.1007/s12206-009-1126-5. Retrieved from: http://link.springer.com/10.1007/s12206-009-1126-5

[3] KIM, J. K. and LEE, C. S., 2013, Fatigue life estimation of injection mold core using simulation-based approach. *International Journal of Automotive Technology* [online]. 2013. Vol. 14, no. 5p. 723-729. [Accessed 20 February 2018]. DOI 10.1007/s12239-013-0079-y. Retrieved from: http://link.springer.com/10.1007/s12239-013-0079-y

[4] KENNEDY, Peter and ZHENG, Rong, 2013, *Flow analysis of injection molds*. 2nd edition. Cincinnati : Hanser Publishers. ISBN 978-1569905128.

[5] KULKARNI, Suhas., 2017, *Robust process development and scientific molding: theory and practice*. 2nd ed. Cincinnati : Hanser Publications. ISBN 978-1-56990-586-9.

[6] Autodesk Knowledge Network: A rich repository of more than a million contributions from Autodesk, its community, and its partners, [online], [Accessed 24 May 2018]. Retrieved from: https://knowledge.autodesk.com

[7] ZIENKIEWICZ, O. C., TAYLOR, Robert L. and ZHU, J. Z., 2013, *The finite element method: its basis and fundamentals*. Seventh edition. Amsterdam : Elsevier, Butterworth-Heinemann. ISBN 978-1856176330.

[8] Thermoplastics vs Thermosetting Plastics, 2014. *Recycled Plastic: The number one source for recycling facts, news and connections* [online], 2014. [Accessed 31 May 2018]. Retrieved from: http://www.recycledplastic.com/index.html%3Fp=10288.html

[9] BENRA, Friedrich-Karl, DOHMEN, Hans Josef, PEI, Ji, SCHUSTER, Sebastian and WAN, Bo, 2011, A Comparison of One-Way and Two-Way Coupling Methods for Numerical Analysis of Fluid-Structure Interactions. *Journal of Applied Mathematics* [online]. 2011. Vol. 2011, p. 1-16. [Accessed 03 June 2018]. DOI 10.1155/2011/853560. Retrieved from: http://www.hindawi.com/journals/jam/2011/853560/

[10] VLK, Miloš, 1992, *Dynamická pevnost a životnost*. 2., přeprac. vyd. Brno : Vysoké učení technické.

[11] SHIGLEY, Joseph Edward, MISCHKE, Charles R and BUDYNAS, Richard Gordon, 2010, *Konstruování strojních součástí*. Brno : Vysoké učení technické v Brně. Překlady vysokoškolských učebnic. ISBN 978-80-214-2629-0.

[12] HASSAN, M. A., MEHAT, N. S., SHARIF, S., DAUD, R., TOMADI, S. H. and REZA, M. S., 2009, Study of the Surface Integrity of AISI 4140 Steel in Wire Electrical Discharge Machining. In : *Proceedings of the International MultiConference of Engineers and Computer Scientists 2009*. Hong Kong : IMECS. 2009. ISBN 978-988-17012-7-5.

[13] ÖZERKAN, Hacı Bekir, 2018, Effect of electrode polarity on fatigue life in EDM. In : *MATEC Web of Conferences: 01107* [online]. Turkey : ICMTMTE. 2018. [Accessed 04 February 2019]. Retrieved from: https://doi.org/10.1051/matecconf/201822401107

[14] EKMEKCI, Bülent, 2007, Residual stresses and white layer in electric discharge machining (EDM). *Applied Surface Science: A Journal Devoted to Applied Physics and Chemistry of Surfaces and Interfaces* [online]. 2007. Vol. 2007, no. 253p. 9234—9240. [Accessed 04 February 2019]. Retrieved from: http://dx.doi.org/10.1016/j.apsusc.2007.05.078

[15] Uddeholm Vanadis 4 Extra SuperClean datasheet, 2018. In : *Uddeholm* [online], 2018. [Accessed 05 February 2019]. Retrieved from: https://www.uddeholm.com/czech/cs/products/uddeholm-vanadis-4-extra-superclean-2/

[16] RŮŽIČKA, Milan, 2000, *Pevnost a životnost letadel*. Praha : České vysoké učení technické. ISBN 80-01-02254-4.

[17] CAMPUS: a material information system for the plastics industry, 2019. [online], 2019. [Accessed 08 April 2019]. Retrieved from: https://www.campusplastics.com/

[18] KUJAWSKI, Daniel and LK TEO, Joshua, 2017, A Generalization of Neuber-s Rule for Numerical Applications. In : *Procedia Structural Integrity 5 , Funchal: 2nd International Conference on Structural Integrity*. Madeira, Portugal : Elsevier. 2017. p. 883-888. ISBN 9781510848566.

8. List of abbreviations, technical terms, symbols and units used

Core shift	A spatial deviation in the position of the core from its original position in the mold before plastic is injected into the cavity.
FSI	Fluid-structure interaction.
CAE	Computed Aided Engineering.
COPQ	Cost of poor quality, these costs would disappear if products and processes were perfect, example could be money spent on tooling repairs.
EDM	Electric discharge machining, material is removed by a series of discrete electrical sparks in the machining gap between the electrode and the workpiece. An important variant of EDM applies thin wires to generate small gaps in the workpiece.
SLS	Selective laser sintering.
EMEA	Region that includes Europe, the Middle East and Africa.
TPM	Total productive maintenance, a system of maintaining and improving production, it focuses on keeping all equipment in best working condition to prevent breakdowns etc.
$R_{p0.1}$	Yield strength of a material for 0.1% of plastic deformation. At this value of stress the material starts to deform plastically.
$R_{p0.2}$	Yield strength of a material for 0.2% of plastic deformation.
R_m	Ultimate tensile strength of a material. At this value of stress the material breaks.
ε_f	Strain at fracture of a material. At this value of strain the material breaks.
S_2	Fluidity, reciprocal of viscosity $[\mathrm{m}^2\,\mathrm{s}^{-1}\,\mathrm{N}^{-1}]$.